APPLICATION OF SLITTING METHOD FOR MEASUREMENTS OF COLD ROLLING RESIDUAL STRESSES

A MASTER'S THESIS

in

Manufacturing Engineering

Atilim University

By

DOĞAN KIVANÇ AKSUNGUR

SEPTEMBER 2018

APPLICATION OF SLITTING METHOD FOR MEASUREMENTS OF COLD ROLLING RESIDUAL STRESSES

A THESIS SUBMITTED TO
THE GRADUATE SCHOOL OF NATURAL AND APPLIED SCIENCES
OF
ATILIM UNIVERSITY
BY

DOĞAN KIVANÇ AKSUNGUR

IN PARTIAL FULFILLMENT OF THE REQUIREMENTS FOR THE DEGREE OF
MASTER OF SCIENCE

IN
THE DEPARTMENT OF MANUFACTURING ENGINEERING
SEPTEMBER 2018

Approval of the Graduate School of Natural and Applied Sciences, Atılım University.

_____

Prof. Dr. Ali KARA

Director

I certify that this thesis satisfies all the requirements as a thesis for the degree of Master of Science.

_____

Prof. Dr. Engin S. KILIÇ

Head of Department

This is to certify that we have read the thesis “Application of Slitting Method for Measurements of Cold Rolling Residual Stresses” submitted by “Doğan Kıvanç AKSUNGUR” and that in our opinion it is fully adequate, in scope and quality, as a thesis for the degree of Master of Science.

_____

Dr. Öğr. Ü. Caner ŞİMŞİR

Supervisor

Examining Committee Members

Doç. Dr. A. Hakan ARGEŞO _____

Dr. Öğr. Ü. Caner ŞİMŞİR _____

Dr. Öğr. Ü. Orkun ÖZŞAHİN _____

Date: 20.09.2018

I declare and guarantee that all data, knowledge and information in this document has been obtained, processed and presented in accordance with academic rules and ethical conduct. Based on these rules and conduct, I have fully cited and referenced all material and results that are not original to this work.

Name, Last name: Doğan Kıvanç AKSUNGUR

Signature:

ABSTRACT

APPLICATION OF SLITTING METHOD FOR MEASUREMENTS OF COLD ROLLING RESIDUAL STRESSES

Aksungur, Doğan Kıvanç

M.S., Manufacturing Engineering Department

Supervisor: Assoc.Prof.Dr. Caner Simsir

September 2018, 77 pages

It is known that cold-rolling residual stresses are associated with certain defects and affect the performance of succeeding manufacturing operations. Because of that, raw material manufacturers try to reduce those stresses by some post-treatments such as stretching and pressing. Determination of through-thickness residual stress profile is important for the design of both the rolling and stress relaxation treatment. This information can also be useful in the design of common manufacturing operations such as bending, and welding and it can be acquired by several residual stress measurement techniques such as neutron/synchrotron diffraction, slitting, contour method etc.

In this study, slitting and ring-core methods have been applied to measure through thickness stress distribution on rectangular bars cut by wire- Electrical Discharge Machining (w-EDM) from a cold-rolled and stress relaxed AA 5083 plate. The compliance matrix for slitting method is derived using Finite Element Analysis (FEA) and calibration matrix for ring-core method is acquired from [1]. The results indicate a good agreement while the slitting method slightly over-estimates the stresses due to neglection of transverse stresses according to assumed cold rolled stress profile. In addition, residual stress measurements were made with the ring core method to confirm the stresses obtained with the slitting method. Measurements with the ring-core method were done up to the quarter of the maximum thickness of 20 mm. Under the circumstances, the residual stress profile due to slitting and ring-core methods was observed to be similar for a certain depth.

Keywords: Residual Stress, Slitting Method, Aluminum, Cold Rolling, Ring-Core

ÖZ

SOĞUK HADDELENMİŞ PLAKALARDA KALINTI GERİLMELERİN ÖLÇÜMLERİ İÇİN YARIK AÇMA YÖNTEMİ UYGULAMASI

Aksungur, Doğan Kıvanç

Yüksek Lisans, İmalat Mühendisliği Bölümü

Tez Yöneticisi: Doç. Dr. Caner Şimşir

Eylül 2018, 77 sayfa

Soğuk haddeleme kalıntı gerilmelerinin bazı hasar mekanizmaları ile ilişkilendirildiği ve sonraki üretim işlemlerinin performansını etkilediği bilinmektedir. Bu nedenle, hammadde üreticileri bu gerilimleri gerdirme ve presleme gibi bazı işlemlerle azaltmaya çalışırlar. Kalınlık boyunca kalıntı gerilme profilinin belirlenmesi, hem haddeleme, hem de gerilme giderme proseslerinin tasarımı için önemlidir. Bu bilgiler, bükme ve kaynak yapma gibi yaygın imalat işlemlerinin tasarımında da yararlı olabilir ve nötron / sinkrotron kırınımı, yarık açma, kontur yöntemi vb. gibi çeşitli artık gerilme ölçüm teknikleriyle elde edilebilir.

Bu çalışmada, soğuk haddelenmiş ve gerginlikten arındırılmış AA 5083 levhadan işlenen dikdörtgen plakaların kalınlığı boyunca kalıntı gerilme dağılımını ölçmek için yarık açma ve halka delme yöntemi uygulanmıştır. Yarık açma yöntemi için uyum matrisi, Sonlu Elemanlar Analizi (SEA) kullanılarak türetilmiştir ve halka delme yöntemi kalibrasyon matrisi [1] 'den elde edilmiştir. Sonuçlar, iyi bir soğuk haddeleme gerilme profili ile paralellik göstermekle birlikte, yarık açma yöntemi, varsayılan soğuk haddelenmiş gerilme profiline göre enine gerilmelerin ihmalinden kaynaklanan gerilmeleri biraz fazla tahmin etmektedir. Ek olarak, gerilmelerin dilme yöntemi sonuçlarını doğrulamak için halka delme yöntemiyle kalıntı gerilme ölçümleri yapılmıştır. Halka delme yöntemle yapılan ölçümler, maksimum 20 mm kalınlığın dörtte biri derinliğe kadar yapılabilmiştir. Bu koşullar altında, yarık açma ve halka delme yöntemleri arasında kalıntı gerilme profili belli bir derinlik için paralel olarak gözlenmiştir.

Anahtar Kelimeler: Artık Gerilme, Yarık Açma Metodu, Alüminyum, Soğuk Haddeleme, Halka Delme.

To My Family…

ACKNOWLEDGMENTS

The author would like to express sincere gratitude to his supervisor, Assoc. Prof. Dr. Caner Şimşir for giving opportunity to work with him on this research, and also thank for his encouragement, guidance, and support during the research.

The author would like to express his deepest and special appreciation to his managers, Dr.-Ing Feridun ÖZHAN, Dr.-Ing Hamdullah MERDANE and Turhan SAVAŞ at ORS Bearings Inc. for their encouragement, guidance and support. The author also would like to express his gratitude to his colleagues, Ozan MÜŞTAK, Zeren ÖZGENECİ, on behalf of all ORS Bearings Inc. members, for their encourage, interest, help, support and technical assistance.

The author has performed all his studies in Metal Forming Centre of Excellence (MFCE), therefore he would like to thank to chairman of MFCE Assoc. Prof. Dr. Besim BARANOĞLU.

The author would like to express his thank to Yahya TUNÇ, Serap YILMAZ, Rasim Köksal ERTAN and all other members of Metal Forming Center of Excellence for their valuable technical assistance, help and support during this research.

The author owes his deepest gratitude to his parents, Sevim AKSUNGUR, Mustafa AKSUNGUR and his brother Öğünç AKSUNGUR for their gentle love, inspiration, support and guidance throughout his life. The author owes his deepest gratitude to his wife Damla AKSUNGUR for her continuous support and patience during this period.

Finally, the author would like to offer his regards and blessings to all of those who supported him in any respect during this research.

TABLE OF CONTENTS

LIST OF TABLES

LIST OF FIGURES

LIST OF ABBREVIATIONS

2D: Two Dimensional

3D: Three Dimensional

FE: Finite Element

FEM: Finite Element Method

FEA: Finite Element Analysis

EDM: Electrical Discharge Machine

σ: Normal stress

σ_x: Normal x-axis stress

σ_y: Normal y-axis stress

σ_z: Normal z-axis stress

τ: Shear stress

λ: X-ray Frequency

XRD: X-Ray Diffraction

SAE: Society of Automotive Engineers

ASTM: American Society for Testing and Materials

ND: Neutron Diffraction

SG: Strain Gage

GL: Grid length

D: Distance

E: Young Modulus

ν: Poison Ratio

C_{ij}: Compliance Matrix

C_{ij}^{1}: Back Face Strain Gage Compliance Matrix

C_{ij}^{2}: Front Face Strain Gage Compliance Matrix

ε: Strain

a: Cut step

a_i: Incremental Cut Step

$P_j(x)$: Legendre Polynomial

A_j: Coefficient Matrix

x,y,z: Cartesian Coordinate Axis

r, Ø, z: Cylindrical Coordinate Axis

φ(phi): Angle between a fixed direction in the plane of the sample and the projection in that plane of the normal of the diffracting plane

K_{Irs},: Stress Intensity Factor

CHAPTER 1

INTRODUCTION

In this thesis study, a series of numerical and experimental studies were carried out on 20 mm thick cold-rolled AA 5083 plate to measure the cold rolling residual stress profile by slitting method. In order to calculate the residual stresses by slitting method in the numerical section of the study, the necessary compliance matrix is derived from the "forward" solution techniques by optimization of various finite element models (FEM) for convenient compliance matrix. In the test section, the data obtained with the strain gage placed on the sample and the data were calculated with the compliance matrix to measure the residual stress profile through the thickness.

Although the work on residual stresses is quite old, the slitting method can be seen as a new method of measuring residual stresses. Related to the slitting technique, parts with residual stresses are cut step by step with a cutting method such as EDM (Electrical Discharge Machine) or sawing machine (to measure the residual stress profile along the depth) [2]. The slot in the terminology describes the progression of the cut along the depth. Strain and displacement measurements along the depth are performed at each step. With the slitting method, only the normal residual stress profile can be measured throughout the thickness with slits perpendicular to the normal stress component.

The cold rolling process in which the residual stress profile is to be investigated using the slitting method is a process where the metal passes through the rolls at temperature below the recrystallization temperatures 450°C. This process increases the yield strength and hardness of the metal by strain hardening which means the crystal structure of the metal is created hardened microstructure for further slip planes. Because the metal is at room temperature, it is less easily processed than a metal above its recrystallization temperature. In Figure 1 the cold rolling process is shown basically to demonstrate the process. This makes the cold rolling process a more labor-intensive and expensive process than the hot rolling process. Due to the selected material, the hot rolling process is excluded from the scope of this thesis.

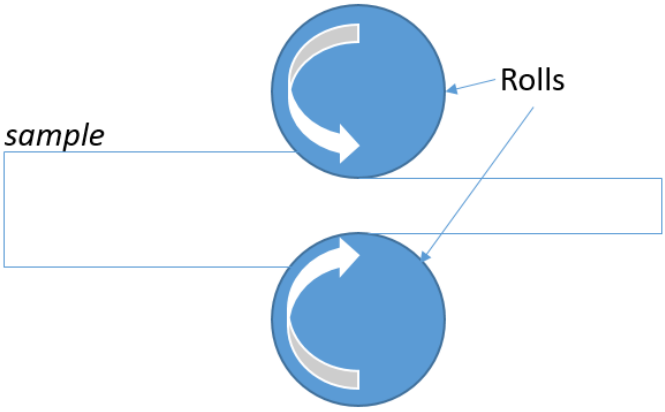

Figure 1: Cold rolling process

Aluminum is selected to study residual stress measurements with slitting method which is the most widely used non-ferrous metal and one of the most abundant of all elements in the Earth's crust. Due to its properties such as low density, formability, corrosion resistance; it has a wide range of application areas like automotive, construction, aerospace and aviation, marine, medical and food. Aluminum products are classified into three categories according to their production technique: extruded, rolled and cast aluminum products. Like aluminum itself, rolling it also has a very short history, whereas the last decades are the rolling technology is matured. Since demands and aluminum industry are growing continuously, the need for producing faster and more efficiently pushes the rolling lines to increase their productivity. Together with productivity, high quality; specifically, consistency in thickness, low flatness, and proper surface appearance are expected to be superior in the competitive environment.

In addition to the visual quality of the materials, the internal stresses occurring during and after the production process greatly affect the working life of the part. The visual quality of the materials, the internal stresses that occur during or after the production process are of great importance. Residual stresses are stresses that exist in the material when there is no external load on the part. Mechanical deformation which is applied to the material during processing can cause residual stresses. For example, inhomogeneous heating or cooling processes result in thermal stress changes in the part, while plastic deformation causes non-matching deformation

mechanisms and causes discontinuities in deformation under temperature variation due to unequal thermal expansion limits. Along with the internal properties of the material, the effects and interactions of the external mechanical or thermal processes, the formation and changes of the residual stress mechanisms in the material can be observed. The state of the residual stresses is related to both the mechanical action from both the previous processes that has been carried out the history of the part and to the stamping characteristics with the deformation. Residual stresses are associated with and are important in fatigue, wear, creep, tensile corrosion cracking, fracture, buckling and failure mechanisms of many mechanical components, especially in parts under dynamic loads. Even if the part is not under external loads, residual stresses induced in the part can be caused by dimensional imbalance after any heat treatment is applied to the part after machining.

While new methods are being developed for the measurement of residual stresses, currently active residual stress measurement methods and research studies and applications are performed. While it is not possible to obtain stresses directly with conventional stress measurement methods, strain or displacement values are measured then stress is calculated from strain or displacement data as a proxy. As a result of the measurements, mathematical calculations are executed using the obtained representative/proxy data to define the stress profile. To calculate the stresses due to external load, the stress values can be calculated by a simple process such as multiplying of the measured strain by the Young's Modulus of the material. Otherwise, when the residual stresses are not caused by external loads and are locked in the structure, these stresses are self-balancing and may complicate the problem in the course of carrying out the required mathematical calculations [3][4]. Residual stresses which are not directly formed in the material and also in balance can be found in the literature studies. Measurements on such materials may show less accurate results than residual stress measurements generated by the external load application. As a result of the measurements used in the relaxation techniques, material is removed from the sample to measure the residual stress distribution. Material removal from the sample also results in a rebalancing of the residual stress distribution in the structure. At this stage, the balancing of the stresses is also taken into account in the measurements. There is a need for detailed and comprehensive calibration to measure residual stresses through proxy measurements using breakage

and other methods. When ultrasonic and magnetic methods are used as examples of other methods, a very detailed calibration is required for the material to be measured. Contemporary, small contaminated grains inside the material can severely negatively affect residual stress for measurements. The measurement accuracy of the stresses of the part coming from its past cannot be measured accurately compared to stresses caused by the external loads. It is necessary to pay attention to residual stress measurement, and it is also important to make a decision between the measurement accuracy and the measurement resolution. In general, these two features measurement accuracy and resolution are mutually contradictory. As a result of these needs it means to reduce the measurement accuracy to make more area scanning, or in contrast to the high resolution in a small area. Metering accuracy is improved by averaging, but at this stage it tends to reduce spatial resolution. Conversely, improved spatial resolution requires measurement of small differences between data on nearby measurement points. Small errors in the measurements made and differences cause large errors and consequently large stress evaluation errors. For this reason, making multiple measurements and using techniques such as average or smoothing can provide simultaneous progression in both desired characteristics. In this context, because of the advantage of non-destructive methods, multiple measurements and reproducible measurements can be taken.

Since, there is no general method for residual stress measurement, the choice of method depends on the size and the material of the part. A table summarizing some general interpretations of residual stress measurement methods in the literature is presented below Table 1. Because of the broad application variety of the methods shown on the table and the implementation of the various methods listed, an attempt has been made to create a master guide. If it is difficult to make any formal verification of the validity of many of the methods used, a criterion has been drawn up as a set of experimental estimates derived from the application numbers and the literature is used. Precise estimates in the second column of Table 1 show the possible measurement accuracy of the different methods.

Table 1: Residual stress measurement techniques and scales [2]

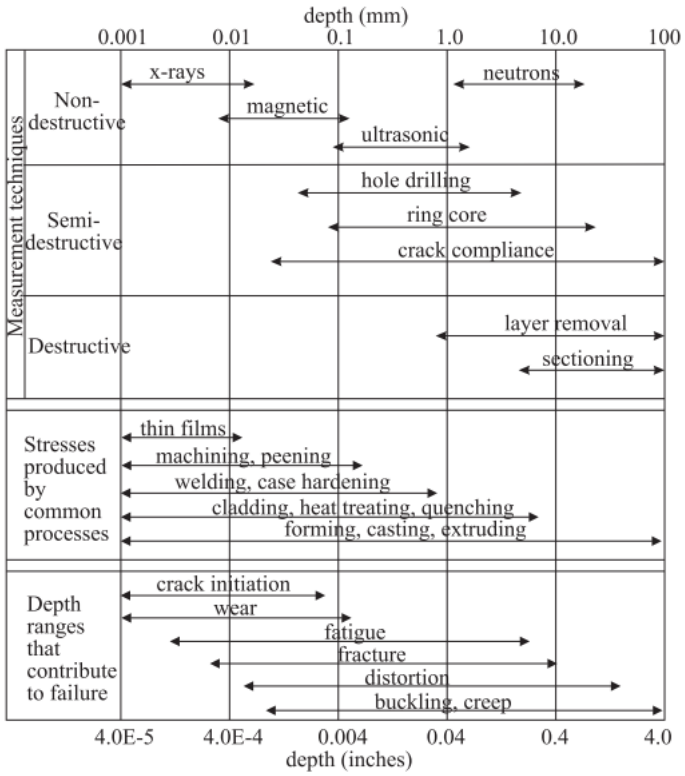

Due to the "locked" characteristics of residual stresses in the literature, it is reported that the evaluation of the evaluation is independent from the measurement technique. Measurements are indirect, even in the case of stresses caused by external loads on the part; a proxy such as strain or displacement is measured to interpret the stresses in the part. The measurement strategy recommended in the literature is the application of comparative measurement techniques and the detection and measurement reasons of the measurement when there is no external load on the part. At this stage, it is not a matter of simply removing and applying residual stresses from any structure. The complexity in this case is that the residual stress measurements must be made on the nearest location due to the destruction of the material containing the residual stress. In the non-destructive measurement techniques which will be mentioned in the following subtopic there is no need to remove any material. Some of these methods require a "stress-free" reference state so that some of the residual stress measurements can be performed and interpreted on a hard layer. This involves difficulties to make it reliably due to the necessity of a reference state. As a consequence of all these difficulties for residual stress

measurement, the measurements of residual stresses typically fail to achieve accuracy and reliability. For this reason, while the various residual stress measurement methods are mature and used on a limited accuracy and measurement range basis, these measurement ranges are often not very large.

When sources in the literature are examined, the structural deformations caused by the variations of the stresses in the structure and redistribution when the residual stresses are relaxed by cutting or material removal are shown in Figure 2 and Figure 3. The resulting deformation mechanism "relaxation" characteristically exhibits an elastic behavior, and there is a linear relationship between the dimension of deformation and the magnitude of the released residual stress. Observation of this basic deformation behavior forms the basis of "relaxation" methods for residual stress measurement [5][6][7].

The methods of measuring residual stresses as a result of deformation measured by cutting the material are described as "destructive" methods on following subtopic. Several "relaxation" methods for measuring residual stresses have been developed over the years for both generic or special samples. Despite the great differences in geometry and experimental technique, all methods are presented with a brief summary of methods for a series of relaxation methods for the concept of deformation by local cuts in stressed material.

Figure 2: Cracking in a cast aluminum ingot due to excessive residual stresses[8]

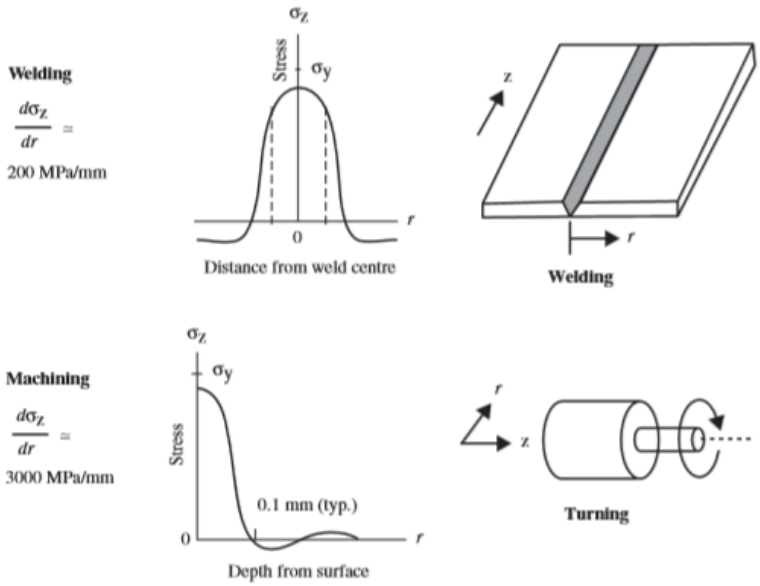

Figure 3: Schematics illustrating typical residual stress gradients induced by various manufacturing process [8]

1.1. Nondestructive Measurement Methods

On the other hand, diffraction methods for residual stress measurements allow non-destructive measurement procedures. With non-destructive measurements, after the residual stress is measured than the stress areas are evaluated, the component can be returned to service and continue to operate. Therefore, the equipment that performs the measurements is developed in a compact way so that it can be carried easily. The Figure 4 is shown general radiation diffraction within a crystal structure.

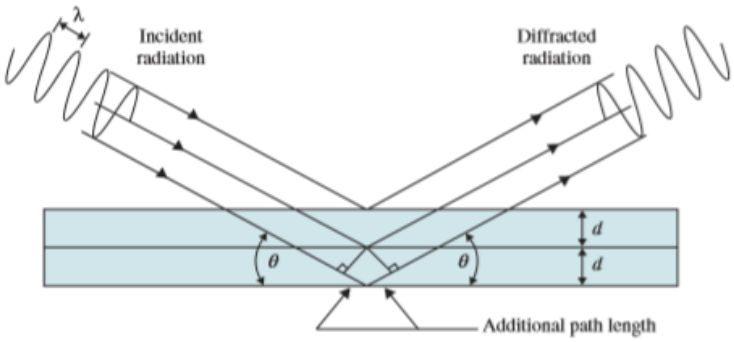

Figure 4: Radiation diffraction within a crystal structure [8]

1.1.1. X-Ray Diffraction Method

X-Ray diffraction (XRD) techniques from diffraction methods perform the strain measurements in the region of the irradiation by measuring the cage spacing of the atoms. In this area SAE International has published a manual on XRD stress measurement [9].

1.1.2. The Synchrotron Method

The diffracted molar energy varies with strain, which is the change in the lattice interval and is measured by an energy dispersive x-ray detector. The Synchrotron method has become possible with advances in detector technology that provide better sensitivity in energy measurement [10].

1.1.3. The Neutron Method

The Neutron Diffraction (ND) method can also perform the measurement of elastic strains caused by residual stresses in the volumetric from the thickness components ranging from 0.1 to 1.5 meter with a spatial resolution of less than one mm. The ability of this method is that it does not require any layer removal attempts. As in the XRD method, the ND method also relates to the gap between the nodal and crystallographic planes of the scattered radiation. These voids are related to residual stress distributions in the structure. The accuracy of the ND techniques requires that the unstressed lattice spacing of the crystallographic planes measured are precisely known because the stress state is in principle and tri-axial depth which this term defines a volumetric measurement unit. As in the case of the synchrotron method, the stress free lattice spacing at the voltage measurement point should be known but it could not be easily measured. This problem is further exacerbated by the fact that the element composition and thus the lattice spacing varies considerably within a component made from an alloy. Additional constraints require that the component is to be brought to a neutron source, each strain measurement requiring more than several minutes to hours, and a single stress measurement of the component in a small gage volume (in the order of a cubic mm) requires at least three hours. Therefore, measurements with ND method is costed higher. However, the ND methods have been applied to residual stress measurements at welding, rolled bars,

plastic deformed plate [11], rocket casings, [12] and many other types of components.

1.2. Destructive Measurement Methods

1.2.1. Splitting Method

The "splitting method" [13][14], as can be seen again in Figure 5, which is presented as an example below, can be caused by the presence of excessive residual stress in the construction material. Basically, a slit is formed on the sample as shown in Figure 5 **(a)** and can show the magnitude of the opening or closing gap on the depending on the residual stress. This method is particularly prevalent in the rapid and comparative realization of quality control in the material production process. This method can also be shown in Figure 5 **(b)** as an example of applications for use in tube geometries to evaluate circumferential residual stresses.

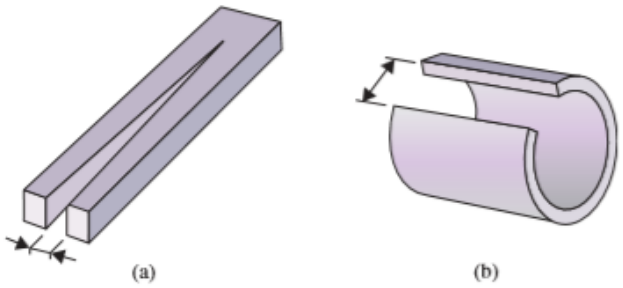

Figure 5: The splitting method (a) for rods and (b) for tubes [8]

1.2.2. Sectioning Method

In the case of residual stress measurement on the sample by the "sectioning method"[15][16], measurements can be made by reading the change in the strain by connecting the strain gage on the cut part or by performing a residual stress measurement by diffraction methods over the cut part. Stress losses, measured with each part cut, provide a valuable data source where both residual stresses before size and original residual stresses can be determined before the cut. Figure 6 shows an example where a sequence of cuts was made to evaluate the residual stresses in an I-beam.

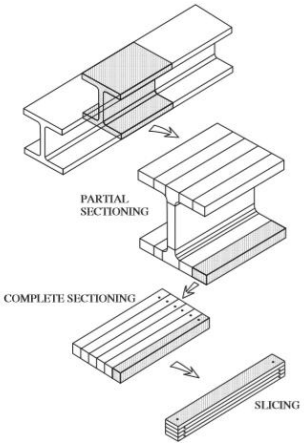

Figure 6: Sectioning method [17]

1.2.3. Layer Removal Method

Another method of destructive measurement, layer removal [15], involves observing the deformation caused by removal of a number of layers of material. This method applies to plates and cylindrical specimens where the residual stresses vary significantly over the surface but are evenly spaced and parallel to the surface. **Figure 7** presents illustrations of examples of layer removal method (a) application on a plate and (b) application on a roller. Since the method uses a strain gage to measure the deformations on the face as the parallel surface layers are removed from the opposite surface from which the measurement is taken.

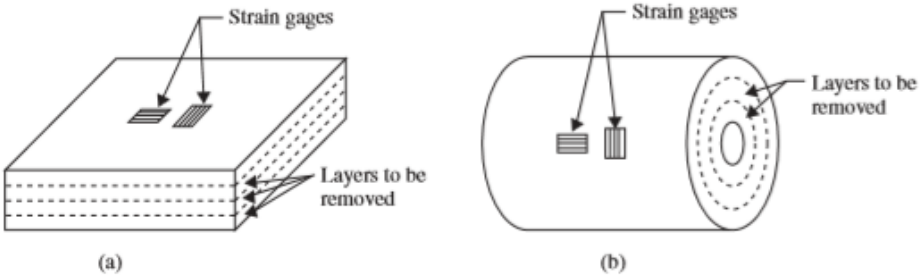

Figure 7: Layer removal method (a) flat plate and (b) cylinder [7]

1.2.4. Hole Drilling Method

Another layer removal method is the hole drilling method [17], which is the most commonly used method of relaxation measurement of residual stresses. In practice, layer removal measurements can be carried out using a small hole drilled on the

surface of the sample and conventionally using a strain gage, or new techniques as optical measurements by the image processing technologies. The hole drilling method which is shown in Figure 8 **(a)** is popular in the industry, and it can provide reliable and fast results with many sample types. Due to the fact that the measurement is destructive, the damaged location is small. By the way, this local damage can also be tolerated and the specimen takes back to its service life. The measurement process has become a standardized procedure with well-defined ASTM E837 [18][19] and valid residuals defined along the depth and through the hole diameter drilled.

1.2.5. Ring Core Method

The Ring-core method[20][21] is similar to hole-drilling method. Unlike the ring-core method, holes are drilled from the outer circumference of the glued gage. The Figure 8 (**b)** shows geometry of the method's implementation. The ring core method has the advantage of larger surface strains than the hole drilling method and allowing larger residual stresses to be measured and reached deeper. Besides, it creates more damage on the sample and has more difficulties in practice.

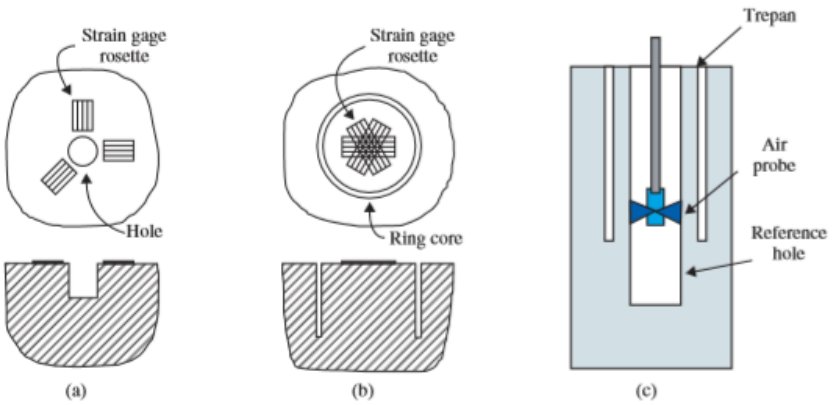

Figure 8: Hole drilling methods: (a) conventional hole-drilling method, (b) ring-core method and (c) deep-hole method [8]

1.2.6. Deep Hole Drilling

The deep hole drilling method [22][23] can be explained as a combination of the techniques of hole drilling and ring-core methods mentioned above. The deep hole

drilling method performs the residual stress calculation by measuring the diameter change in the hole along the hole depth. In Figure 8 (**c)** shows an application of deep hole drilling method to the specimen. The purpose of this method is to allow deep internal residual stresses to be measured. It is known to be applied especially in large steel and aluminum casting blocks.

1.2.7. Contour Method

The Contour Method [24][25] shown in Figure 9 **(a-c)** is mentioned in the literature as an improved technique for making full residual stress measurements. This method involves cutting the sample section using wire EDM and calculating the surface height of the cutting surfaces using coordinate measuring devices or surface hill distance meters. As shown in circle in Figure 9 (b), the surface of the material is deformed (outward protrusion for compression stresses, which must be pulled inward in the grooving). Residual stresses existed at the material after the cut essentially can be evaluated from the finite element (FE) calculations by determining the stresses needed to return the deformed surface to flat surface as plane. In practice, surfaces on both sides of the cut are measured and the mean surface height map is used to avoid any effect of the measurement asymmetry. The contour method is remarkable because all the material gives a 2D map of the residual strain distribution on the section. Figure 9 (d) shows an example of axial residual stress response which was calculated according to strain distribution on the cross-section of a railway track [26].

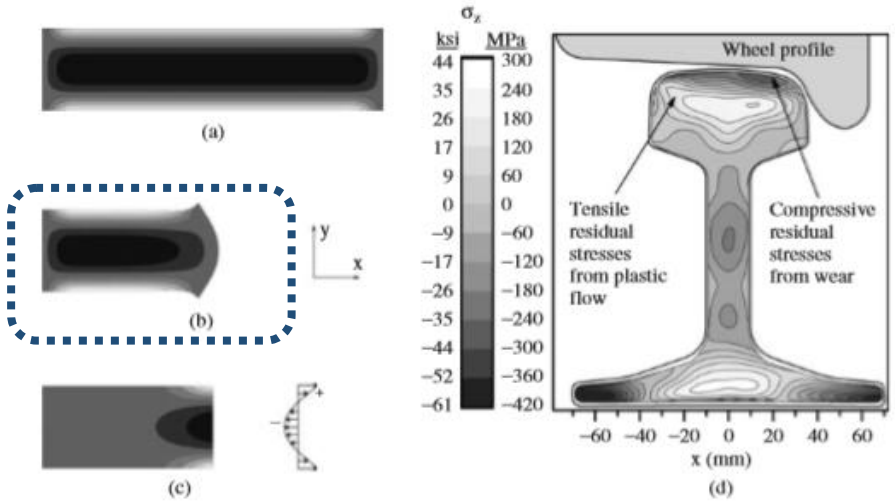

Figure 9: Contour Method (a) original stresses, (b) stress-free after cutting, (c) stresses to restore flat surface and (d) measured stress profile of a railway rail [8].

After providing brief information on destructive and nondestructive methods for residual stress measurement, residual stress profile of cold rolled plates measurement study by slitting method is selected as a subject in this thesis study. Particularly in the cold rolling process, residual stresses occur as a result of the deformation of the material passing between the rollers. In cold forming process, if the roll diameter is selected small as a result the thickness reduction per station cause to deform the metal small which is shown in Figure 10 (**a)**. Otherwise, if the reduction area of the rolled is a large according to a number of rolls per station, the surface of the cold rolled plate is deformed as shown in Figure 10 **(b)**. As noted above, the diameter of the work roll is a very important factor affecting the overall properties of the roll mill. Detailed studies for high or low rolling rates have been carried out by H. Watabane, H. Honjo and K. Miyasaka [27].

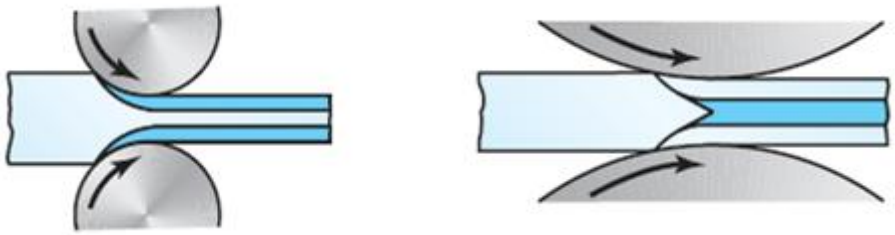

Figure 10:(a) Residual stresses developed in rolling with small diameter rolls or at small reductions in thickness per pass. **(b)** Residual stresses developed in rolling with large diameter rolls or at high reductions per pass; note the reversal of the residual stress patterns [28].

A number of destructive and nondestructive measuring methods can be used to achieve residual stress measurements on cold rolled aluminum plates throughout the thickness. Non-destructive measurement methods are started with surface measurements by XRD method. To measure the deep residual stress, it is necessary to remove the material from the surface. With this method, after a certain depth, the residual stress profile cannot be measured properly because of the validity of the XRD method in the literature is up to 600 microns. Other nondestructive methods, such as the synchrotron and ND methods, can be used to measure cold rolled residual stresses in the thick plate. Since these devices are in limited laboratories, due to the time and budget problems, nondestructive methods might not be preferred. Therefore, it is necessary to make a choice from the damaged methods for the

measurement of residual stress in cold rolled plates. Ring-core and the deep hole drilling methods, which are mentioned briefly in the introduction section, can be used for the measurement of residual stress along the thickness of cold rolled plates. However, these methods also require depth limitations and the need for equipment for application.

1.2.7. Slitting Method

The slitting method, developed in Los Alamos laboratories is used by research centers and engineering firms all over the world to measure residual stress in structural materials such as welded plated, pressure vessels and so on.

In this thesis study, the residual stress profile of the 20 mm cold rolled AA5083 material will be calculated by using the slitting method. With the slitting method, the compliance matrices specific to the plate geometry have been obtained by using "forward" solutions for residual stress calculations. The FEM was used to obtain the Compliance Matrix and a series of model studies were performed to confirm both the FE mesh structure and the size of material to be removed from the plate. As a result, there is a need to increase the number of experiments and to obtain a sufficient number of test specimens from the plate of the size 400x400x20 mm. Therefore, it is planned to perform a study using the finite element method to find the optimum test sample length. Thus, the size that provides the minimum residual stress relief on the test samples to be cut from the large plate will be preferred. Figure 11 shows a slitting method schematically.

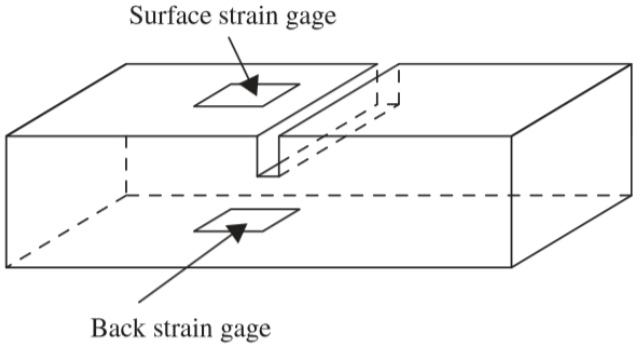

Figure 11: Slitting Method

CHAPTER 2

THEORY OF SLITTING METHOD

Method was originally developed by Finnie and et al. [29][30][31][32][33]. A detailed review work has been carried out by Prime [2] and a monograph compilation for the method which is referred to as "crack compliance method" or "compliance method" in the literature [34]. However, in order to accurately define the concepts in this respect, ASTM Task Group E28.13.02 proposed which this method is to renamed as a "slitting method" to emphasize the parallels between slitting and hole drilling methods. The slitting method provides a great benefit for residual stress measurements in practical laboratory conditions because the application procedure is easy and quick, and reproducibility is excellent [35]. In this part of the thesis study, it is aimed to provide a minor transfer from the extensive technical background in the literature. Useful information summarized in [2] and [34] has been utilized when conducting measurement-oriented studies.

For slitting method, there is a resource which is created and maintained by M. B. Prime on the internet [36]. In this method, depth is increased by forming stepwise planar slits on the material retaining the residual stress. The deformations around the slit are caused by the redistribution of the residual stresses on the slit surface, the measurement is taken by the strain gage which is placed back face of the plate. And the measurement is taken as a function of increasing slit depth through the thickness of the plate, and is used to determine the residual stresses present on the slit planes before cutting. In this chapter, the slitting method application procedure for measuring the residual stress through the thickness of the plate by positioning strain gages on the aluminum plate is shown as Figure 12. In this thesis the slitting method will be used to measure the residual stress profile of the cold rolled aluminum plate. The cutting process is started from the origin coordinate axis of the plate to the y-axis direction. The method also has the flexibility to enable the measurement of residual stresses in various materials other than metals such as glass, crystal and plastic, and to measure various geometries such as blocks, beams, plates, rods, tubes and rings [37,38][14][39][40][41][42][43][44]. In a typical application for metallic materials, the slot is cut using a wire electric discharge machine "wire-EDM" [45], and the

measurement of the strain relaxation was made using strain gage and data acquisition device. Slitting method requires a transformation matrix for residual stress calculations. This matrix is called compliance matrix. For forward solutions, it is necessary to create a compliance matrix for the sample to be measured by using the final elements method. The compliance matrix is formed by strain distributions obtained as a result of finite element analysis. The strain gage location planned to be bonded to the test sample to form the compaction matrix and the location of the strain data to be read as a result of finite element solutions should be made from the same location. [39,40,42,46].

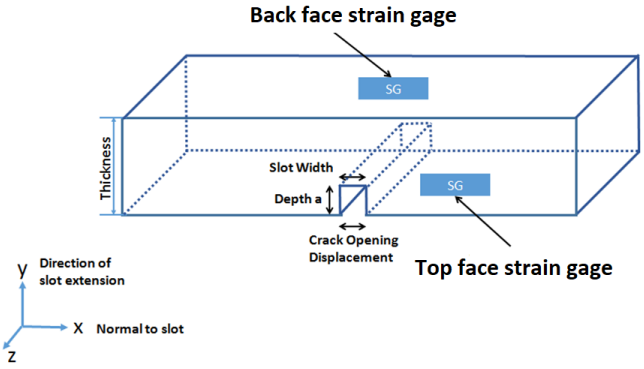

Figure 12: Schematic of the Slitting Technique

In the tests carried out with the slitting method, data were collected from the backface with strain gage as a result of slits formed throughout each thickness. The graph of strain data read from the backface against the depth of cut along the thickness is presented in Figure 13.

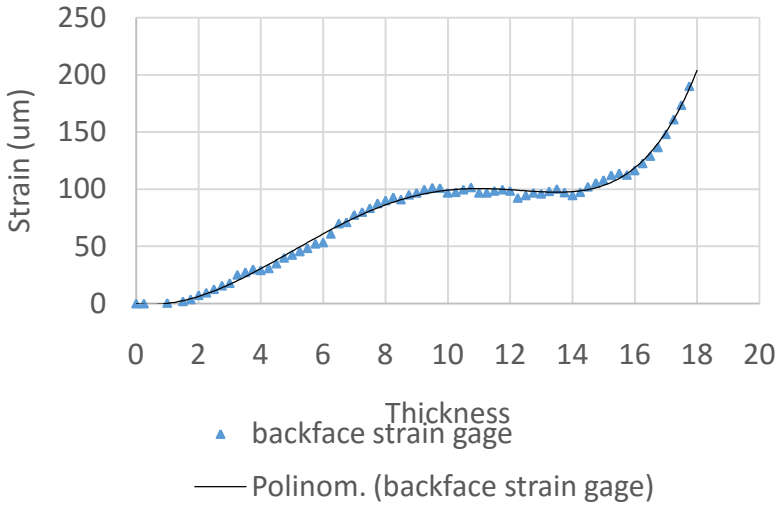

Figure 13: Slitting method strain measurement from backface and polynomial fit.

The normal stress component of the slot formed on the surface is measured. Figure 13 shows also the normal stress component σ_x. At the same time, with the slot opening, the two shear stress components are also being relaxed in τ_{yz} and τ_{xy}. At the point where the slot is cut, the presence of shear stresses influences the measured normal component of strain values and related stress components.

First, the shear stress component in the structure will have a geometrically minor effect on the x-axis strain values measured by the strain gages on the surface. In its essence, Cheng et al. [33] conducted studies to determine the shear strain values on the surface rather than measuring the normal strain values in the studies they performed. In their study, they empirically determined the relationship of $e_y = (y\text{-}\nu_z) / E$ by the surface strain gage. The local shear stresses only affected the shear strains. The shear stresses loosening around the slot have only a small effect on the strain gage compared with normal stress component. For this reason, rosette-type strain gage is used in the hole-drilling method which could be explained as the positioning of 3 normal strain gages with different angles to each other. In addition, the gages are placed in the middle angle of x and y-axes used to measure shear stresses which do not directly affect the strain measurements.

In addition, in the case of the free surface, the shear stresses at the edges of the part must be zero. It is unlikely that these tensile values will reach a significant value unless they have an extensive distribution in the z-direction at the split slot. Since the method of drilling holes can be easily applied, this situation is not valid for the same case. In the literature on crack compliance, shear stress is discussed more frequently with the thought that x-y components may interact. The effect of the shear stresses in the sample in the residual stress measurement by the slitting method is the result of the small scale of the effect of the studies. Here, with the free surface condition, the shear stress must be zero on the top surface where the shear starts. For this reason, it is negligible for near-surface measurements using crack compliance or hole drilling. For residual stress measurements through the thickness, τ_{xy} is not considered negligible. In this regard, Cheng and Finnie [47] showed that the residual shear stress component had no effect on the normal strains on the backface.

The calculation of residual stresses is based on the superposition principle which assumes strain data is due to elastic behavior. If the residual stress distribution in the

structure is known, the strain relief which will be formed by any cut can be easily calculated. The FEM software can also be used for forward calculation. However, in the process of finding an unknown residual stress profile, a number of basic functions representing residual stresses through the thickness must be used.

Legendre polynomials were used to represent residual stresses in the analyzes to be carried out in this thesis study, as in many studies in the literature which is shown in Figure 14. The Legendre polynomials called Legendre functions of the first kind, Legendre coefficients, or zonal harmonics (Whittaker and Watson 1990, p. 302), are solutions to the Legendre differential equation. The Legendre polynomials $P_n(x)$ are illustrated below for $x \in [-1,1]$ and $n=2,..,12$. The Legendre polynomials are orthogonal over (-1,1) with weighting function 1 and satisfy where δ_{mn} is the Kronecker delta in Equation 1.

$$\int_{-1}^{1} P_n(x)P_m(x)dx = \frac{2}{2n+1}\delta_{mn} \qquad (1)$$

In order to calculate the unknown residual stress profile in the material, after determining the coefficients of the series distribution with the help of Legendre functions, matrix multiplication is performed. Another reason for choosing Legendre polynomials is that they could provide force and moment balance throughout the section. This balanced along the residual stress measurement thickness could be defined as the equation of the force with the following Equation 2, and the equilibrium with Equation 3 which Ψ is dummy variable for the integrals.

$$\int_{-t/2}^{t/2} \sigma(\psi)\, d\psi = 0 \qquad (2)$$

$$\int_{-t/2}^{t/2} \sigma(\psi).\psi\, d\psi = 0 \qquad (3)$$

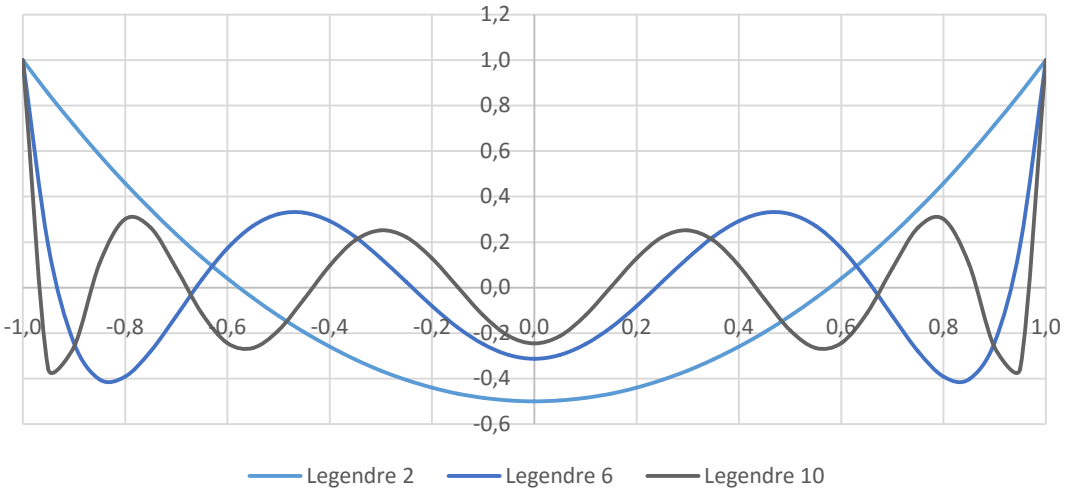

Figure 14: Legendre Polynomials Distribution Graphs

In order to calculate the coefficients in the linear equation system, matrix inversion operations were performed. As shown in the Figure 15 which summarizes the slitting method, the strain reading will vary depending on the depth of cut in the according to strain gage grid length. The reason for this change in the strain is the residual stress relaxation in the longitudinal section of the material.

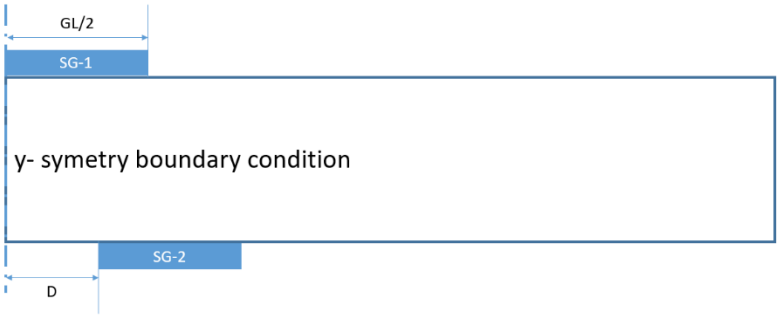

Figure 15: Strain gage positions on to the specimen and fem.
SG: strain gage, GL: grid length, D: distance

As a result of the analyzes carried out by finite element method, residual stress distributions were applied by Legendre polynomials. Cutting analyzes were performed by means of element removal method and analyzes were performed to change the residual stress distribution in the specimen. As a result of these analyzes, the strain changes that occur according to the residual stress distribution in the structure were obtained. This calculation method is called "forward" solution in the literature [42]. Thus, according to the representative strain distributions generated by the Legendre polynomials, strain variation is obtained at each cutting step. As a

result of this calculation, C_{ij} coefficients are obtained. Which is shown in Equation 4 compliance matrix equation which is generated from the FEA.

$$C_{ij} = \varepsilon(a = a_i, \sigma(x) = P_j(x)) \qquad (4)$$

To obtain all the elements of the C_{ij} matrix, the calculations are repeated for all Legendre functions 2^{nd} to 12^{th} order and all cutting depths. The behavior of the material during the experiment is assumed elastic and each measurement will be approximately equal to a linear combination of the results from the forward solutions as the (a_i) depth measure and (ε^i_m) strain measurement is defined as Equation 5.

$$\varepsilon_i^m \approx \sum C_{ij} A_j = \varepsilon_i \qquad (5)$$

Here, the inverse of the linear equation system matrix is calculated to find the A_j coefficients containing the unknown amplitudes with the aid of each Legendre polynomial. Zero strain cases are excluded to avoid uncertainties in the formation of the compliance matrix. In order to obtain the matrix A_j defined as the coefficient vector in the equation, the solution of the equation system is needed. Thus, the residual stress distribution can be calculated according to known stretching functions. Thus, the residual stress profile in the material before cutting can be calculated by solving Equation 6.

$$\sigma(x) = \sum A_j P_j(x) \qquad (6)$$

In the slitting method (crack compliance) applications, A_j coefficient matrix is calculated from the least squares method as in Equation 6. The number of strains measured during the cutting operation at the forward solution exceeds the number of Legendre polynomial orders. For this reason, estimation and distribution of residual

stress profile is required. Therefore, two basic approaches have been carried out in the simplification process of the problem in the method of performing the calculations with finite element method. These are respectively, first it is assumed that the residual stress state is two-dimensional (2D). Second, residual stresses are estimated throughout the entire section of the specimen. Residual stress does not cause any external forces in the relaxation process, but requires that the net force and torque generated by the displaced ε(x) strain in the plane is zero. This is why the main advantage of using Legendre polynomials to solve these problems is that the polynomials in the first and second order are balanced when they are excluded [48]**.** If the first two orders are excluded initially, then the sequence will be performed with a distributed stress polynomial of n-1 terms. For this reason, the estimated strain will also provide a balance. It is also possible to use more than one strain gage to increase the sensitivity of the slitting method Figure 15. The extra measuring location provides a two-way signal acquisition through the thickness, thus providing an important advantage by improving the calculation results of the linear equation system to reach the results from two-sided strain gage data to generate combined compliance matrix**.** Where two strain gages are used, the compliance matrix for both measurements must be combined in an improved and segmented system as in Equation 7 compliance matrix equation for multiple strain gage measurement

$$C_{ij} = \frac{C_{ij}^{1}}{C_{ij}^{2}} \qquad (7)$$

with corresponding measured strain vector as shown in Equation 8 compliance matrix equation for multiple strain gage measurement in strain definition.

$$\varepsilon_i^m = \frac{\varepsilon_i^{m,1}}{\varepsilon_i^{m,2}} \qquad (8)$$

An inverse solution is found with Equation 9 to calculate the residual stresses in the strain distribution measured by cutting through the thickness of the cold rolled plate. The number of Legendre polynomials we used in our study stress distributions is 10

and the number of strains measured for each cutting step through the thickness is 90. The least squares fit is applied under these conditions.

$$A = \left[\left(\underline{C}^T \underline{C} \right)^{-1} \underline{C}^T \right] \varepsilon \sim m \qquad (9)$$

In the above equation, the bars under the letters represent matrices, and the ones in the as subscript of the letters represent the vectors. The expression between square brackets is the pseudo-inverse and provides an approximate solution. Among the strains are calculated using Equation 9, root mean square error between the measured and fitted strains [49]. The coefficients of the A vector obtained by the solution of the equation are found. Then the A vector is processed for residual stress distribution calculations with Legendre polynomials.

$$\sigma(x) = \sum A_j P_j(x) \qquad (10)$$

Equation 10 was again used in the calculation of the residual stress profile by slitting method. Here we have been able to calculate the A_{ij} coefficients in Equation 6 with the aid of the C_{ij} (compliance matrix) obtained by further residual stress profile calculations. With the obtained A_{ij} coefficients, coefficients of residual stress distribution at the cross section can be expressed by Legendre polynomials. A code was generated for the mathematical calculation to reach the residual stress distribution calculation with slitting method which was placed in Appendix 1.

Finally, the obtained A_{ij} coefficients were written as coefficients in the Legendre polynomials and the residual stress profile was obtained across the thickness with the help of the series expansions. Due to the number of data in this calculation, a code was written in MatLAB program to perform these calculations.

Common practices for method of adaptation can be divided into several different components. The method has analytical, experimental and practical differences. On the other hand, there is a balance between accuracy, precision and ease of application of various cases. There are usually two components for the analytical part of the adaptation method which can be expressed as forward and inverse solutions. In the forward solution phase, successive solutions can be defined as the answer to the

question of strains (displacements or KIs) that are gradually cut and measured from a specimen with a known residual stress distribution. These strain distributions are functions of the depth of the slot being opened and are called adaptation functions. The problem that arises here can be solved in general by using fracture mechanics, FEM or other numerical solution techniques. Secondly, the aim of the inverse solution is to find the residual stress distribution that actually coincides with the measured strains. This problem can be solved by using the advanced solution and then by using more complex inverse solutions, such as the average residual stress calculation in each increment of the depth in series expansion. This will significantly affect both the accuracy and depth resolution of the measurement results.

As a result of, it seems that a simplifying superposition principle is used to solve the forward problem. When a slit or crack is imparted to a part containing residual stresses, some of the stresses are released and the overall stress distribution is rearranged. Each slit made to the depth of the profile is inserted to the results of the rearrangement combined with the previous step. At this stage, a solution to trace the deformations must be determined. Therefore, researchers used Bueckner's superposition principle [50], originally developed for fracture mechanics. This principle, shown in Figure 16, indicates that deformations can be calculated by considering the fracture body and by loading the fracture surfaces on the unbroken body to the original residual stresses present in this plane. It is possible to implement a further solution without using the superposition principle. Perl and Arone [51] performed material removal to calculate deformations after thermal loading and an application to represent residual stresses in the FE model. As an approach, using the FE software residual stress formation is modeled as an initial condition for the specimen. Then the elements could be removed from the specimen in order to simulate the removal of the material cut. With this approach, we need to make sure the finite element model (FEM) does not result in an excessive strain distribution or deformations after the first solution step. Because the residual stress state of the structure must be balanced and the deformation must not occur in order to maintain the balance. In the analysis of the FEM, the first step should be provided to perform the calculations required to reach the balance. The state after this step should be considered as unmodified and the subsequent analysis steps should be modeled to simulate slot trimming.

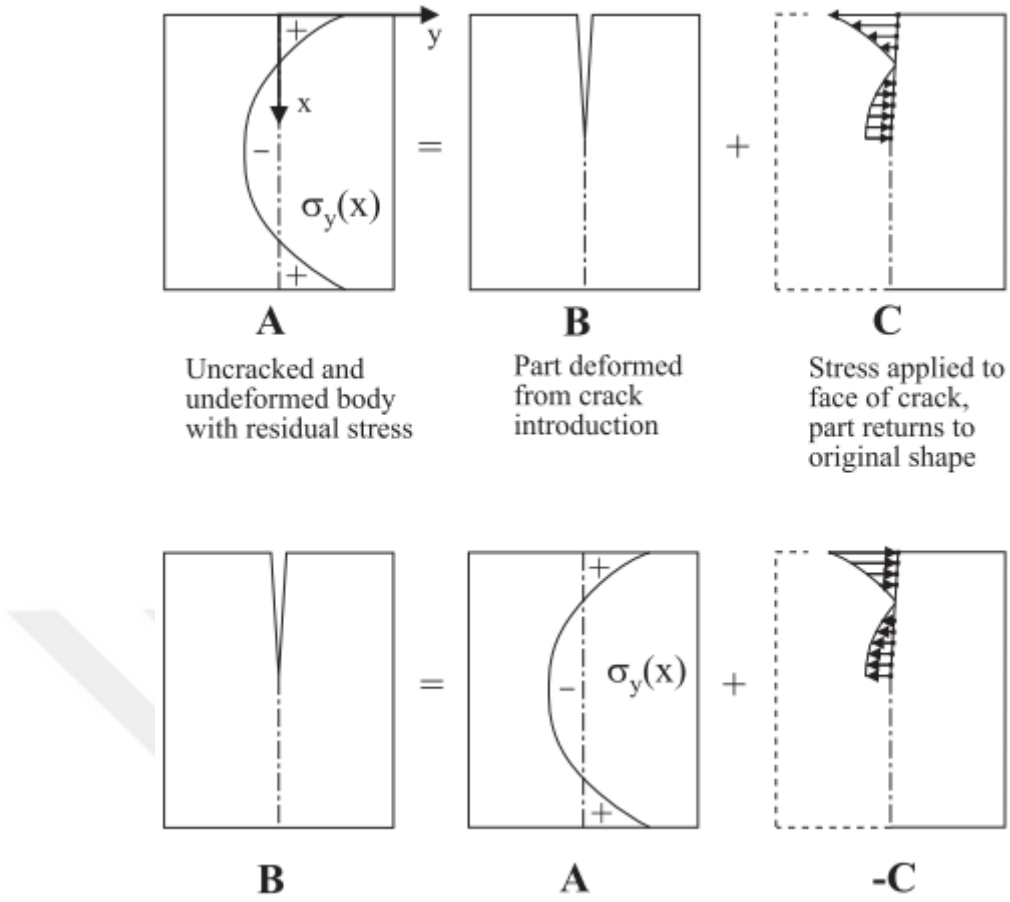

Figure 16: Superposition principle used to calculate deformations from releasing residual stresses [2].

To determine which method should be used in the literature to calculate a new forward solution, the FE solution is foreseen as a system which needs to be fast for a single test and to be able to create a strategy that allows easy simulation of the slot section with removed boundary condition of each element. Investigation of the slitting method suggests that there is no need for special mesh at the crack tip. For many tests on similar geometries, the programming of fracture mechanics, body power, or other numerical solutions can save time in the long run. For a new geometry, in addition to the existing solutions, there are complications on the solution of the weight functions of the fracture mechanics [52][53]. In this section, the application of the weight function solutions to the crack compliance measurements is reported. If there is no solution for a similar geometry or if the geometry is not complex, an FE solution can be applied. The FE solution is again the best choice for close-up surface measurements where the width of the progression

and the shape are important. It is also not a final expanse of all K_I solutions but additionally, the review clearly states that solutions lead to strains or displacement.

As a result, by using the FEM for the slitting method, the geometry specific compliance matrix, in which the residual stress measurement is carried out, can be carried out quickly with forward solutions. Each step progresses in a series of steps during which the boundary conditions at the node points are released during the symmetry recovery corresponding to a given slit depth to represent a certain slit depth. In this study, detailed study results of the slit depths and the model of the FE created will be given in chapter 4 in the derivation of compliance matrix. In FEM, Legendre polynomials were applied and FEA were performed and strain results were collected for each cut step. Thus, the compliance matrix is determined for a strain gage size where the results of the displacements provided by the multistage FEA are obtained.

CHAPTER 3

LITERATURE SURVEY

The literature survey has been carried out for the slitting method of the residual stress profile formed on the cold rolled aluminum plate subject to this study. The literature review is basically divided into two main sections. First, the literature survey for the slitting method, which forms the basis of the study, has been carried out with other methods which can be used for residual stress measurement in cold rolled thick plates. The theory and application studies about slitting method which is the subject of the thesis are also included.

Yoshihiro Nakayama and Tetsuya Takaai, Shinichi Kimura's studies on surface residual stresses in cold rolled 5083 aluminum alloy are investigated by XRD procedure. As a result of this study, it was determined that measurements with XRD did not have a similar measurement capability as strain gage application. According to residual stress estimates made by diffraction on the surface of the samples, no obvious effect of the reduction of the thick stress area on the texture was found. In the study, the residual stresses found out on the cold rolled sample surface along the rolling direction exhibited both tensile and compressive properties. These stress profiles have been found to show a tendency to decrease with the depth.

In XRD measurement of the residual stress distribution in cold rolled 5083 aluminum alloy, the residual stress calculations in the cage structure were carried out on the basis of the Reuss [54] model. Based on the existence of macroscopic and microscopic stresses here, information has been found about the mechanisms which cause residual stresses during cold rolling of 5083 aluminum alloy. As a result of this study, it was found that the cold rolled 5083 aluminum alloy has a linear relation between the cage strains. In addition, there is a linear relation between the applied unit stress and $\sin^2\varphi$. Thus, it has been determined that the measured values of the cage strains show good agreement with the values calculated according to Reuss's model while another deduction was made that the macroscopic residual stresses measured at 30% cold rolled samples were added to the microscopic residual stresses.

In another study of cold rolled 5083 aluminum alloy, changes in XRD elastic constants affected by the diffusion plane were experimentally investigated. It has been found that the elastic constants of the XRD are closely related to the variations of the density, which is influenced by the formation of the rolling texture. Some discrepancies have been observed between the measured values by applying the XRD method with the elastic constants measured by mechanical procedures. The x-ray elastic constants, when considering the dependence of the other x-ray elastic system on the fracture flatness and the planes, decreased with the decrease in the reduction in the cold rolling.

Residual stress measurements have been carried out over the rolled 7050-T74 material over the thickness where the measurements have been made using the crack compliance method. The unexpected features encountered in this study has been asserted as the cause of the crystallographic structure.

After this step, the literature review reveals that the slitting method is a stable measurement technique used on thick plates. The literature survey on the compilation of studies on the theory of the slitting method and the following examples are presented from different applications and the adaptations of the slitting method.

3.1. Studies on Development of Slitting Theory

The crack compliance method has also been used to determine near-surface tensions [33]. For residual stress measurement, a calculation model with normal and shear stresses near the surface with the application of non-deep cuts called as the crack compliance method has been proposed. It has been shown here that the optimum zones for strain measurement have been obtained and compared to the conventional hole drilling method. Their study with a finite body whose dimensions are related to global variables has aimed to obtain process and material independent numerical analysis.

M. Gremaud, w. Cheng, I. Finnie, and M. B. Prime [33] conducted an analytical background study of "compliance method" for residual stresses measurements from the sub-surface and near-surface. In their study, strain has been measured as a function of tension, residual stresses unknown in previous studies have been

represented by a series of continuous polynomials. From their study performed, partial functions have been used to represent stresses. Errors and slip effects of this method have also been shown in numerical simulations. The method has been presented analytically based on using overlapping "piecewise functions" and the goal has been to establish a general procedure for rapidly varying residual stress distributions. Here, the least squares method has been used to reduce the effects of errors and numerical simulations and measured strains show that the method has been reliable and reliable.

In addition, Hans-Jakob Schnidler and Peter Bertschinger [55] performed measurements on a high-strength steel after cracking and tempering on a rectangular beam. They have developed a method that can automatically calculate the strain distribution according to the resultant measurements using a weight function.

Experimental determination of tensile strength factors due to residual stresses has been studied by H.-J. In the study by Schindler, W. Cheng and I. Finnie [56], an experimental method has been proposed that allows stress intensity factors to be determined directly, without residual tension being pre-determined, depending on the remaining strain. The stress measurements have been taken by means of some basic relationships of the linear elastic fracture mechanics, which are the mathematical connections needed to determine the stress intensity factor. Two examples which allow analytical behavior to be explicitly derived for the geometric system.

It is necessary to know the stress intensity factor which is formed by the residual stress as a function of the crack length for the reliability analysis or the life test of the part. In particular, the tensile strength factor is largely influenced by the Crack Compliance (CC) rather than the residual stress. As shown below, it provides the ability to obtain the Stress Intensity Factor (SIF) directly and accurately without knowing the permanent stress. In fact, calculating the stresses from the SIF instead of the inverse (as in all other methods) is the first of the CC method. In applications where tensile stress factors due to residual stresses are required, the crack compliance method is very simple, as summarized above, because it ensures that the SIF can be detected directly without having to pre-determine the residual stresses, thus guaranteeing high accuracy and reliability.

In particular, the sensitivity to residual stresses is low at small cuts and slit depths, and therefore the stress ratings in this area have more uncertainty than elsewhere. The cut Legendre series is by the piece, i.e., this method reflects uncertainty together with localized relaxation. Regular Legendre and unit pulse methods usually give more consistent results. However, the correction type can affect the tensioning solution in this region by smooth straightening which produces straight line profiles and by straightening which produces horizontally rotating curves. These effects are localized and, in general, both normalization types give satisfactory results. Flat normalization is numerically simpler. As a result, in this study, each of the three stress calculation methods is effective and each has its own specific characteristics. The unit pulse method is conceptually clear and has the best ability to solve steep bending gradients and sharp curves in the cut-depth range. The slit in the uncut area may give reasonable estimates of stretching except the depth, but it does not always have a realistic shape. The regular Legendre method may also give reasonable estimates of stresses beyond the slit depth, but not always realistically. The regular Legendre method has almost the same ability to solve orthogonal bending radii and cut curves in the slit depth. It has a good ability to give a preform to estimates of the stresses in the uncut area. For this reason, the regular Legendre series method is proposed as a general purpose constant stress calculation method for the treatment when the stresses in the uncut area are an estimate. Depending on the shape expected from the edges of the tensile profile, smooth or rough can be used.

The effect of plasticity for increasing shear or crack compliance has been investigated to measure residual stress profiles [57]. On the basis of FE simulations, faults can be strongly associated with the K_{Irs}, which are stress-intensity factors originating from the section extension into the residual stress area. 3D simulations also show that errors are largely dependent on the amount of constraint provided by the piece width. Simulations have been used to develop a procedure to predict errors from the experimental data. Even if there is a possibility of plasticity errors in the measured residual stresses, the K_{Irs} can be easily calculated using only the experimentally measured strain. Calculation is called "open" because flexibility is assumed. After that, the apparent K_{Irs} can be used to limit the errors in the measured residual stresses. The error limit is given as a function of the K_{Irs} which are not resized and the width of the part.

The use of cut methods has been applied to map the residual stress distributions in micron level in amorphous materials [58]. Residual stresses in crystalline or glassy materials often play an important role in the performance of advanced devices and components. Stresses in amorphous materials cannot easily be determined by micron scale diffraction in classical laboratory methods. For this reason, a technical study has been carried out to map the residual stress profile with high spatial definition and a 3x3x25 mm rectangular prism geometry have been used and the Zr-based Zr50Cu40Al10 material was used as the specimen. The acceptable rate of accuracy, which is measured by the stress relaxation digital image correlation. The process has been applied with small balls on the surface and residual stresses calculated by using the FEM. The results from micro cuts generated by micromachining on the surface can often be obtained using a simple analytical model. It has been shown that the cutting method was reduced to micro level in their study.

The works carried out on the residual stresses lead to the name M.B. Prime and has been categorized as relaxation or diffraction method of residual stress measurement techniques using a compilation study conducted by Prime and its team and have advocated a specific technique based on a certain bit category and sometimes their own experience or abilities rather than using the best technique for specific applications. In these studies, sampling have been made by examining the examples that can be invisible from the relaxation and diffraction measurements of the critical stress. A better approach to planning residual stress measurements is to start with a detailed assessment of why stresses need to be measured and how the results are to be used. Only then the most appropriate measurement plan can be developed. The use of multiple measurement types provides the most useful information instead of single measurement technique, which does not lead to the full state of tension especially in challenging sections. The main objective of their work to find the best technique to determine the constant stresses which are important to an objective requires particular aspects. A comprehensive understanding is important to know why they want to know about residual stresses and how to use them. Limited preferences should be abandoned to determine the best way to measure stress and the most sensible approach is to use multiple measurement techniques, containing both destructive and non-destructive [59].

Finally, M. Prime for the incremental cutting method have grouped the steps to follow by performing an experimental procedure study [60].

Ueda and Fukuda [61] examined the use of the FEM to reconstruct relaxed residual stresses after cutting and limited their operation with simple, they had not implement transverse stress concentration at the section.

The method for calculating residual stress with the cutting give results for the stresses in the slit depth range, practical considerations typically limit this range to about 90-95% of the sample thickness. Force and moment balance can provide additional information that can be used to estimate the residual stresses in the "data not available" region within the bond beyond the maximum slot depth [62]. Here, three different numerical methods have been investigated to calculate the residual stress profile through the sample thickness. These are the Legendre series, the regular Legendre series, the edited pulse, the pulse narrower. In a wide range of depths exceeding the maximum depth of the cross section of measurements have been taken on aluminum forgings, the regular Legendre series solution usually gave the most realistic stress results. In the study, they also performed an effective and accurate low-stress cutting operation of EDM [63] with reference to the study is performed. It is an important mathematical challenge to calculate the residual stresses originally from the theoretically measured stresses. There is an inverse problem among the thickness, the residual stress distribution and the measured strains.

3.2. Studies on Development of Slitting Application

M. Beghini and L. Bertini [64] have performed residual stress measurements after flattening with a chip lifting process applied to both surfaces of the plates after laser welding operation, using API 5LX64 ferritic steel plates welded with three different connection shapes. The welded connections of flat plates in different shapes measure the residual stress using the experimental and FEM. In the cutting method, while the front face has started to cut, the other back face was moved to the opposite direction due to the progress. The cut has been resumed and has continued until the piece has been cut. By describing a modeling method for planar residual stress measurements, the sensitivity coefficients evaluated by the incremental sections and FEM in the welded structure have been found and the strains have been experimentally

measured. Stresses have been calculated using the obtained coefficients and verified by the measurements.

Milling, sawing and especially EDM devices are used as cutters in the relieving process for residual stress measurements on buildings. Because the depth of the cuts is known and controlled correctly by EDM, it is used for linear solutions in the reduction of errors. W. Cheng, I. Finnir, M. Gremaud and M. B. Prime [45] have also studied the effects of EDM use and near-surface residual stress measurements. They have used their study on a rectangular beam using 304 stainless steel. The EDM residual stress effect compliance method has been investigated analytically and experimentally. The model developed to estimate the stresses near the surface intercepted by the EDM also showed excellent similarity under different configuration and cutting conditions. In addition, the resulting errors were completed with the least squares method. Exceptional results have been obtained from EDM-induced cuts using a bent specimen as predicted by the tests. In EDM and other layer removal applications, it has been observed that the residual stresses generated by the layering with the cutting tools have matched with the direction of cutting.

In addition to the work carried out on the welded flat plates, a residual stress test has also been carried out for the connections made by stir welding.

The friction applied at low temperature in relation to the welding source is thought to be low at the stresses in the friction stir welding. High rigidity clamps can be used on the plates to be welded, causing internal stresses during cooling and expansion moments. The results of the experiments were qualitative and quantitative, and the effects of parameters such as tool size, welding speed, tool turn have also been examined.

Garry S. Schajer, Michael B. Prime [65] demonstrates mathematical partnership of physically different measurement types and suggests a general approach to residual stress solutions. In addition, it has been shown that the regulation of Tikhonov [66] is an effective way of reducing the effects of measurement noise. This method has been successfully demonstrated using data from the shear (compatibility) measurements and has achieved excellent correspondence with independent residual stresses. The equilibrium constraints have been successfully demonstrated using the data obtained

from the slitting measurements admit the application and the residual stresses determined independently were similar.

Residual stresses have been assessed using the fracture mechanics approach [67], where stresses or displacements measured at a point on the edge of a plate when a new crack was introduced and extended from the edge are used to remove the state of existing stresses. FEA and experiments have shown that this method is valid and effective for measuring the two dimensional residual stress distribution of a welded plate.

The evaluation of the residual stress area by cutting method in weld joints after stir welding of aluminum 2 series T3 saw plates in their work [68]. The plate they apply is rectangular. In the study, residual stress measurements were taken from the welded plate along both sides of the weld and with perpendicular cuts to the weld. For longitudinal test pieces, the socket was placed in two different positions at the center of the weld opening and at a distance of 5 mm from the weld center line, in order to receive the thermomechanical heat affected zone sample. The fracture mechanics approach was used to calculate the residual stresses and the reverse weight function method was used to obtain initial stress values. In the longitudinal direction, the most likely region for fatigue crack nucleation is a peak extensional voltage on the forward side of the thermomechanical / heat affected zone.

A rectangular shaped bar was made on five blocks with a thickness of 17.8 mm, cut from a single 316L stainless steel plate shot with a uniform laser using a cross-section [35]. Unlike other studies, this study presents a reproducible and stable method of study. While EDM cuts were similar to other studies, it was observed that EDM effects were investigated using stainless material in order to better observe these effects and it was also found that this study also provides measurement aimed stabilization. The aim was to study the reproducibility of the cutting method in laboratory conditions, by measuring residual stress measurements on similarly prepared coupon samples, to measure similar residual stress distributions as a function of depth from the surface. Each block was annealed and cut from the larger 316L stainless steel plate which was then smoothly machined by laser cutting. With lasers, the parameters were selected to provide a residual stress distribution that was highly compressed on the raised surface and had a sustained depth of compression.

The standard procedures for the cutting method were examined and the depth profile averages and the surface reached 668 MPa and the applied surface reached 2.9 mm below zero. Standard deviations of 15 MPa and absolute maximum deviations of 26 MPa residual stresses were obtained.

A study on estimations and measurements of fatigue crack growth rates in 2024-T351 beams subjected to plastic deformation bending was presented, in which the fatigue, fatigue and fatigue cracks in the work were carefully controlled to reduce the residual stress factors that could affect the growth rate [69]. Here, the permanent stretch formed by the bending process is characterized by the cutting method and a perfect fit between the two methods is observed. The focused crack growth rates were predicted by three Linear Elastic Fracture Mechanics (LEFM) superposition based methods and compared with experimental measurements. The estimate of the effects of partial crack closure, which is related to the experimental data, is included in the variation normally found in the fatigue crack growth rate test of material which normally does not have residual stress. Thus, if the residual growth is known to be due to the residual growth of the crack growth via the permanent stress fields, the residual properties can be predicted by using the superposition concept as much as crack growth through residual oxidation material, provided that the stress remains balanced during fatigue, material properties cannot be changed by residual stress input. The residual stress fatigue crack significantly affects the growth rates, compressing the residual stress, slowing the crack growth and accelerating the residual stress in the stress. For this reason, material is removed by plastic deformation in order to delay residual stress, delay crack initiation and slow crack propagation. 76 x 76 extruded aluminum 2024T351 extruded bar, 305x36x11 mm middle crack tension specimen was used, and a specimen plastically deformed by bending was used. In contrast to the other articles, a study has been carried out to observe the effects of residual stresses on fracture crack opening on a plate with plastic deformation and containing residual stress. A number of torsion bending processes were used to produce residual stress and were investigated by shear methods. The progress of residual stresses with plastic deformation was examined with a special fracture mechanics study which tried to observe the effects of residual stresses. The three sets of superposition fatigue predictions correlated with the measurement of crack growth through the residual stress field generated by plastic

twisting of the aluminum 2024-T351 beams. The sample was carefully selected and the bending and fatigue loading, such as large plastic yield or residual stress relaxation, was carefully controlled to minimize the factors beyond the residual stresses that could affect the fatigue crack growth rate. The plastic bent beam sample allowed accurate residual stress characterization by a bending method and shear method with an excellent agreement between the two methods. Superposition or modifiable overlay crack growth estimates for intermediate length cracks that are expected to cause partial crack closure have shown good correlation. Top-position contact method, which analyzes the partial crack-closing state, has greatly improved the correlation with the experimental data. In general, the lap tension predicted correlated with the two factors in the rate of crack growth, the fatigue crack in the residual stress-free material is expected to vary with the measurement of growth rates. It is concluding that if the residual growth is known to the residual stress through residual stress areas of the crack growth through these permanent stress fields, the residual stress can be predicted using the concept of superstructure through crack growth by means of permanent stress material provided that the residual stress remains damaged during fatigue, the effect is taken into account.

A study investigating the effect of residual stresses for estimating warpage of aircraft body parts made from aluminum plates [70]. Plate geometry was used in the study and material 7050 T 7451 was used. Volumetric stresses come from the manufacturing process of the plates, where the distortions in the body structures relative to the works in other articles are of two residual stress types. Machining-induced residual stresses are formed below the surface during rapid surface treatment, and these stresses increase while the thickness of plates decreases. In particular, volumetric stresses in the study are aimed at creating a mathematical model for the prediction of the distortions in body structures. It has to be build and test a mathematical model for predicting the multiplication of body components caused by bulk stresses. The scope of work is limited to only hot rolled aluminum plates. Typically, the thickness varies from 6.35 to 153.5 mm on the specified material. The following section on the methodically progressive work presents a good approach.

The mathematical model passed the validity test; no reason was found to justify the rejection of the model, based on the criteria and criteria set for verification. The

magnitude of the pincushion of the thin-walled test pieces typical of the combined body parts made of aluminum plates 7050-T7451, which can refer to the residual stresses caused by the plate production process, did not matter. The main cause of the deterioration was the presence of large residual stresses that entered the surface layer with a chip removal process. For this reason, the reduction of machining residual stresses or the removal of the surface layer by mechanical or chemical means will considerably reduce the deformation. The accuracy of estimates based on any mathematical model is, of course, influenced by the uncertainties in the input data. The greatest uncertainty is related to the distribution of residual stresses on the plate. Since the number of samples available for calibration experiments is small, it is not possible to reliably measure the uncertainty. It can be only presented a subjective assessment without estimating that the maximum degradation estimates based on the procedure described here are within 40% relative error.

In the residual stress measurement, job done on the destructive measurements of the residual stress profiles in the two vertical planes. In residual stress measurements, only one measurement can be taken without affecting successive measurements without stretching release. However, when the initial measurement establishes a tensile profile along an entire plane, the released tensile can be determined by an additional tensile analysis including the results from the first measurement, and then the account can be included in the next measurement. To demonstrate this study, residual stress measurements were made by cutting the coupons subjected to laser shot peening to measure the residual stress profiles of the two vertical planes in aluminum compact pull coupons. For coupons, the measured stress profile in the first plane is used to calculate the released tension in the second plane. By adding this free stress to the measured stress for the second plane, we obtain a tensile profile for the second plane in the original configuration. The results of a numerical model that predicts residual stress due to laser-induced impacts are presented and the results of the model are presented and the agreement between the model and the test results gives confidence to the applied overlay method. Two slit measurements were made on the vertical planes in each of the two laser interrupted C (T) coupons. By combining the released tension in the first shear measurement with the results of the second measurement, it was possible to obtain permanent stress profiles on two

vertical planes in the same shear. Comparing these stress profiles with the results of the simplified matter analysis reassures the applied multilevel method [71].

Residual stress measurements of layered specimens which have some tension discontinuities originated from cutting process may cause permanent stresses. Stress discontinuities in the samples are difficult to measure and can have profound effects on linkage and other failures. Increasing shear, also known as crack compliance, is an excellent solution to solve stress profiles, even when there are usually high gradients. Data reduction for slitting usually involves some roughness, which makes it difficult to resolve discontinuities. In this study, we begin with a new technique for analyzing cut data using Tikhonov regularization and extend this technique to allow for stress discontinuities in material interfaces. the new method is then experimentally demonstrated on several samples including metals and ceramics. The power and flexibility of the modified pulse-regulation method and its ability to resolve discontinuous stress profiles for these tests were limited to experimental issues. In aluminum coated uranium fuel plates, the plates were very wide and the thickness of the layers was not equal. In multilayer ceramics, the sample was bent, but the slits were flat. In any case, it was difficult to know precisely the depth of the knife according to the interface position. For the fuel plates it would have been possible to cut out a test specimen at a finer width without altering the longitudinal stresses and then obtain a better controlled slit depth compared to the interface. For ceramics, we plan to arrange a symmetrical layer and test a new sample without curvature for this reason [72].

CHAPTER 4

DERIVATION OF COMPLIANCE MATRIX

The strategy for calculation residual stress profile from strain reading presumes as elastic behavior which depends on superposition principle. When the residual stress distribution of a material is known, the stress relaxation to be generated which originated from the cutting operation can be calculated. This calculation can be performed using a general purpose FE software. Basic functions representing a series of residual stress distributions along the thickness can be used to find the unknown residual stress distribution in the material. Legendre polynomials, which have a balanced distribution in terms of representing the residual stresses in the structure or thickness, are being used during the formation of the compliance matrix in the residual stress measurement by slitting method. The calculation of the unknown amplitudes of the elastic behavior principle is found by inversing the linear equations. According to the location where the strain gage is placed, the strain variation at each cutting step varies depends on existing stress distribution. Slitting method which is detailed explained in chapter 3, a "forward" solution is found by using a linear elastic equation system [9] and a set of depth calculations are performed. In order to create all the elements of the compliance matrix, the cut-out depth is repeated for all mathematical functions used in the basic function. C_{ij} compliance matrix is defined according to $\varepsilon(x)$ strain function parameters as explained in Equation 11. According to the functions in the equation, the strain values read out as a result of Legendre polynomials, which form the residual stress distribution in the structure, are calculated for each a_i cutting step.

$$Cij = \varepsilon\big(a = a_i, \sigma(x) = P_j(x)\big) \qquad (11)$$

As a result of thesis study, strain data is collected step by step and calculated for each Legendre polynomial to the generation of each element of C_{ij} matrix. The physical problem used in obtaining the Compliance Matrix is studied in 2D. With the cold rolling process of the aluminum plate, the residual stress profile changes along the thickness and the similar profile section along the plate width. For this reason, the problem is considered as a two-dimensional (2D) model according to the thickness

cross-section. Legendre polynomials, which have a balanced distribution in terms of representing the residual stresses in the structure or thickness, are being used during the formation of the compliance matrix in the residual stress measurement by slitting method. Figure 17 shows the geometric approach to solving the problem, the initial stress conditions are created by the Legendre polynomials, and the FEM and boundary conditions for the forward calculations. In the Figure 17, *t* is the thickness, *L* is the length, *x* and *y* demonstrate the two-dimensional Cartesian coordinate system. The compliance matrix obtained as a result of the analyzes contains positive and negative values. It could extract the residual stress distribution by using the values in appendix for any material and thickness. For this purpose, the operator who wants to perform the residual stress measurement is only able to position a strain gage on the test sample and apply the cutting process incrementally.

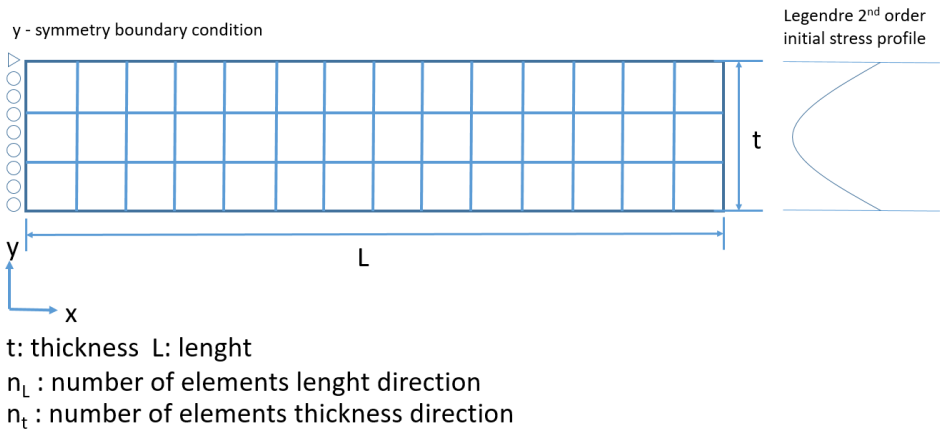

Figure 17: Conceptual demonstration of FEM

In order to identify the problem, the x-axis direction was also selected as the rolling direction. Since the slitting method is applied by cutting, the cut line is regarded as a plane of symmetry. Boundary conditions are applied from the top to the x and y axes to limit the displacement, as indicated in the Figure 17. For other points located on the axis of symmetry, only x axis displacement boundary conditions are applied to fix. The plate thickness is modeled as a 2-unit size in the range [-1,1] where the Legendre polynomials have a balanced distribution, the basic functions of which we apply the section stress distributions. The length of the plate *(L)* was modeled in various lengths, in proportion to the thickness *(t)*, as the ratio *(L / t)* respectively 1/2, 2, 4 which the dimensions of the length variation show in Figure 18. The samples

which were used in the experimental works of this study have a certain distance to keep the rolling residual stresses to a minimum when cut from the plate.

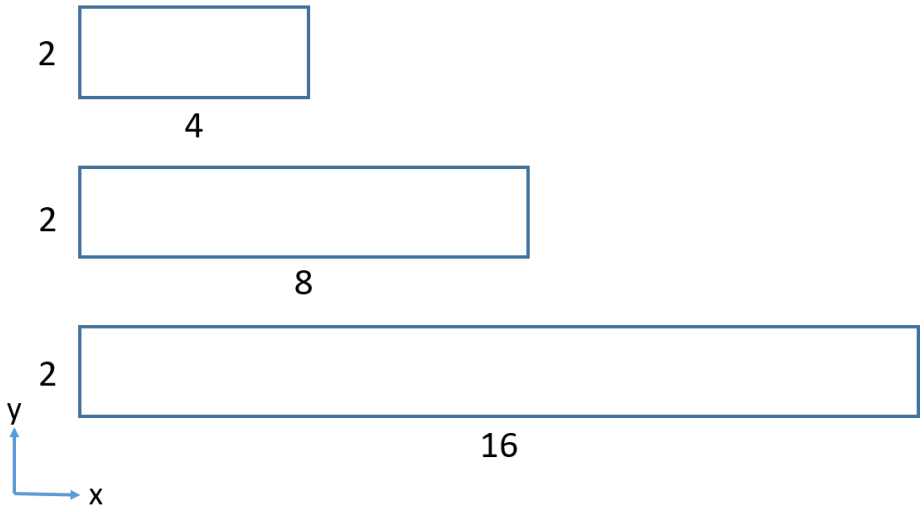

Figure 18: Models used for determination of the effect of specimen aspect ratio.

As mentioned above, 2D dimensionality is considered as the problem definition and plane strain / stress solutions are realized. The linear elastic properties will be used as the material to be used in the calculation of residual stresses. For this reason, the elastic properties of the material are needed because the residual stresses in the structure are elastic stresses. When the literature is examined, studies have been done to investigate the effects of local plastic deformations during cutting process. Plastic stress relaxation states have not been investigated in our study [57], assuming that the plastic stress changes during the cutting and the localization of the relaxations and the dimensional effects of the sample sizes are at a minimum.

Following the physical identification of the problem, the modeling of the FE was performed in the numerical application phase. MSC Marc 2017.1.0 software student version was used for the FEM as in Figure 19.

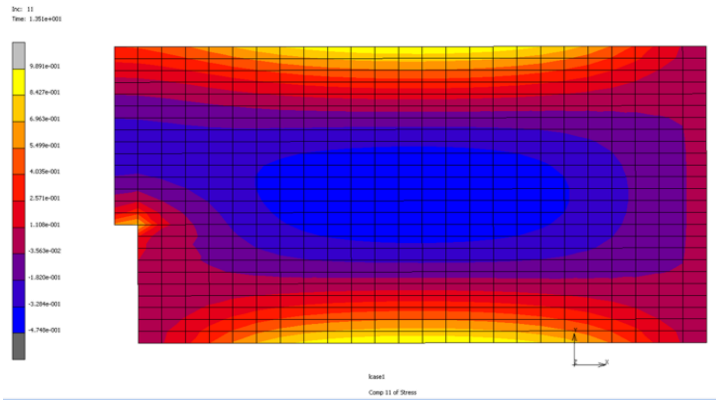

Figure 19: FEM result for axial strain distribution in the specimen at half thickness of the specimen.

The problem is defined as elastic problem using small strain approach. In the analysis, quad element shape is used to form the mesh structure. The software which was used in this thesis study was full integration as quad element and analyzed with element types such as 4 and 8 nodes which is shown in Figure 20 basically. Initial analyzes were performed using a quad element with 4 nodes. As a result of the shear analysis, it was observed that the stress distributions in the center of the edges of the elements needed to be calculated. This leads to an analysis with quad 8 element type which contains the node point as a node in the middle of the edge of each element. Thus, during the shear analysis, strain distributions in the elements were observed homogeneously.

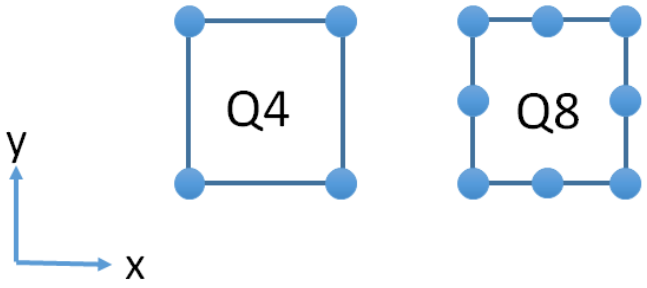

Figure 20: Linear (Q4) and quadratic (Q8) elements used in the study.

The cutting operation was carried out with the aid of the NC machining tool in the MSC Marc software. The NC machining tool is defined only by the definition of a path that requires the cutting path of the cutting tool. NC code steps are defined in

such a way that the cutting tool modeled as in Figure 21 shows the cut through the +y axis in the symmetry axis of y.

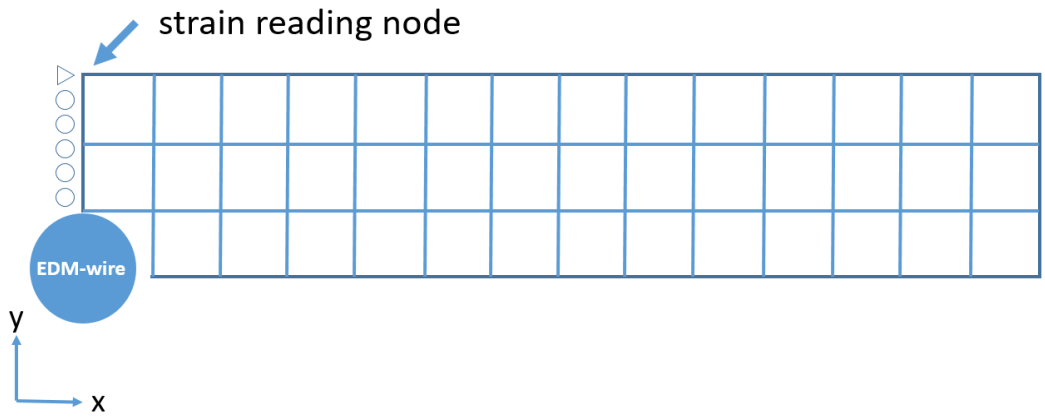

Figure 21: Cutting FEA Demonstration with wire-EDM

In the modeling study, a roadmap for the development of the FEM was followed. Firstly, the section thickness is divided into 25 equal elements. Elements were also created along the length of the plate so that each element would have a size of 0.08 units and an aspect ratio of 1:1 would be preserved. The ratio L / t = 4 for the first model was used as recommended in the literature [1]. In the first analyzes made, it was found that the stress distributions calculated in the elements lifted through the cutting line did not reflect the tensile strength well. In this respect, the transition from element type quad 4 element type to quad 8 element type has been performed.

As a result of the analyzes carried out in Figure 22 the stress intensity distribution on the lifted elements as a result of the cutting analysis is shown for element types Q4 and Q8 as Table 2. The tensile strength is calculated precisely with the quad 8 element type using 8 nodes.

Table 2: Simulation matrix for element selection

1st iteration	25 unit elements through the thickness	Quad 4
2nd iteration	25 unit elements through the thickness	Quad 8

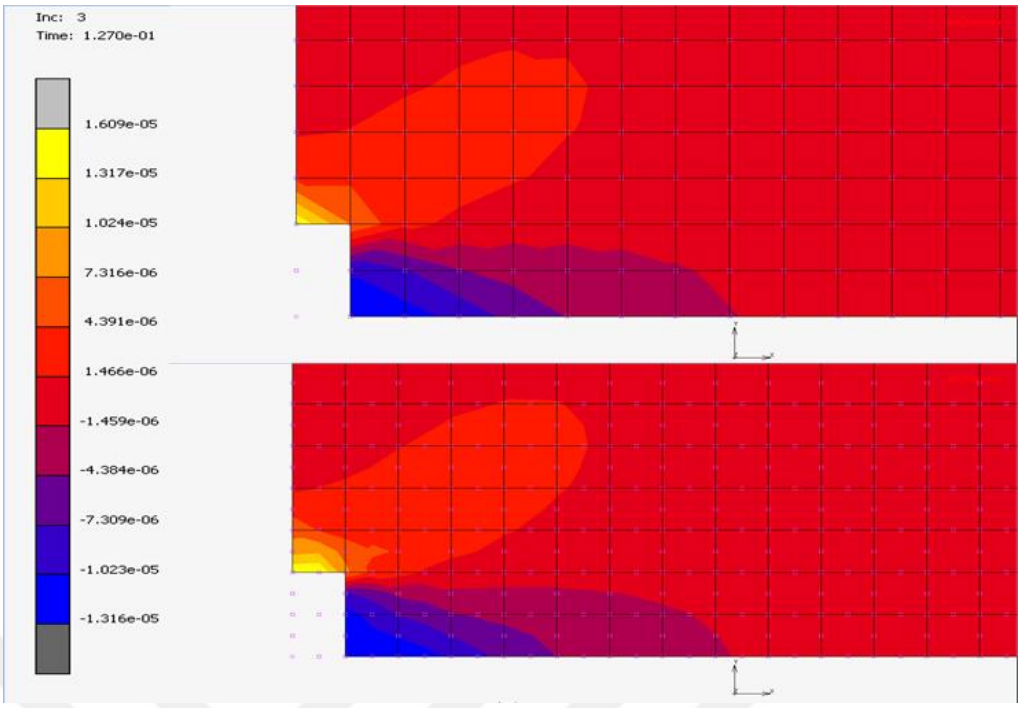

(Quad 4 vs Quad 8 strain distribution results)

Figure 22: Strain distribution according to element selection.

Precise calculation of the tensile strength in each interrupted element is achieved by changing the element type used. This was followed by studies on element density optimization analyzes for plate sections. Here, the plate thickness is 25, 50 and 100 mesh elements, respectively as in Table 3. Thus, while the compliance matrix is being created, measurements taken from the point where the sensor is located are obtained smoothly.

Table 3: Simulation matrix for element density optimization.

3rd iteration	25 unit elements through the thickness	Quad 8
4th iteration	50 unit elements through the thickness	Quad 8
5th iteration	100 unit elements through the thickness	Quad 8

Table.3 shows strain changes in Legendre 2 prestressing according to the number of elements in the cross section of the table.

Table 4: Simulation Matrix Length Optimization

6rd iteration	Length / thickness = 4	Quad 8
7th iteration	Length / thickness = 8	Quad 8
8th iteration	Length / thickness = 16	Quad 8

By means of various FEM, it is aimed to reach the most suitable model parameters to obtain the compliance matrix. The specimen length comparison ratios of FEM are shown in Table 4. First of all, it has been decided to work with 100 elements throughout the section as a result of the work done on the density of elements in the section above as shown in Table 3. For the residual strain measurement, the sample size must be determined according to the minimum residual stress over the sample to be removed from the plates. At this stage, in addition to the literature recommendation, compliance matrices have been derived with FEMs for half the sample rate and half the sample rate in the literature. The compliance matrix strain results obtained from these models were compared with the L / t ratio proposed in the literature and the most appropriate size evaluation was carried out. The table for comparison of models with each other is given below Table 5, Table 6 and the sample sizes for the experiments with optimum model parameters are also reached. As a result of the finite element analysis performed to determine the size of the sample, it was observed that the recommended ratio in the literature was better than the rates we evaluated in our study.

To obtain the required Compliance Matrix for the calculation of residual stresses, FEA was modeled and analyzed by 2D plane strain approximation. In addition, analysis can be performed by the plane stress solution method to solve the problem in order to obtain the compliance matrix. The relationship between the two solution methods is also expressed in the literature as in Equation 12. In order to show that our analysis works parallel to the literature, analyzes are also modeled by using the plane stress solution method in the FE software.

$$\frac{B}{t} > 2.0 \; for \; E' = \frac{E}{1-\nu^2} \qquad (12)$$

In the MSC Marc 2017 program, the geometric properties section was selected as "Structural Plane Stress" and the width of the material was entered. In the analysis, it is necessary to select the appropriate element type for the solution method. For this reason, element type selection has been made in the "element types" menu content as "Planar Solid Structure Element Types" (plane stress full integration - No. 26). On the "Job Parameter" menu, the "Analysis Dimensions" parameter is set to "Plane Stress". Plane stress approach and cut-off analyzes were performed by applying Legendre polynomials with the parameters selected for the analysis. In the evaluation of results, Figure 22 shows the results obtained by using the Legendre polynomial second-level initial stress model for plane strain solution and plane stress solution methods. It is presumed that the main difference between the strain values read from the same point is due to the problem approaches.

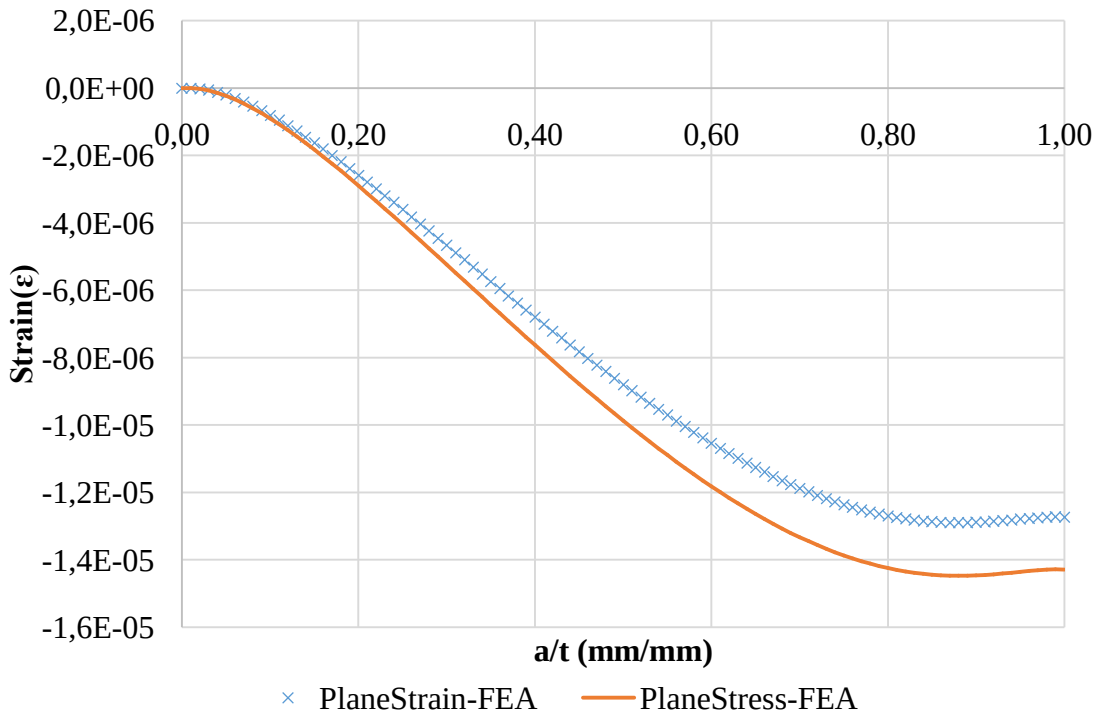

Figure 23: Plane strain vs plane stress results comparison.

Table 5: 4L vs 8L plane strain compliance matrix comparison.

Normalized RMS Error										
3.898E-10										
L2	**L3**	**L4**	**L5**	**L6**	**L7**	**L8**	**L9**	**L10**	**L11**	**L12**
5202984.09	2.59	2.20	2.08	2.02	1.99	1.96	1.93	1.93	1.90	1.89
STDEV										
2.13e-17	9.89e-22	4.78e-19	1.65e-24	4.57e-21	3.68e-25	1.72e-23	1.39e-25	2.78e-25	1.70e-25	1.95e-25
Standard Error										
2.13e-19	9.89e-24	4.78e-21	1.65e-26	4.57e-23	3.68e-27	1.72e-25	1.39e-25	2.78e-27	1.72e-27	1.95e-27
2.13e-21	9.89e-26	4.78e-23	1.65e-28	4.57e-25	3.68e-29	1.72e-27	1.39e-27	2.78e-29	1.72e-29	1.95e-29
Total / Overall Standard Error										
2.129e-19										
Total Standard Deviation										
7.061e-18										
Total Signal / Noise Ratio										
5.520e09										
SE / NE										
100	100	100	100	100	100	100	100	100	100	100

Table 6: 16L vs 8L plane strain compliance matrix comparison.

Normalized RMS Error										
2.251e-10										
L2	**L3**	**L4**	**L5**	**L6**	**L7**	**L8**	**L9**	**L10**	**L11**	**L12**
3.00e03	1.50e-03	1.27e-03	1.20e-03	1.16e-03	1.15e-03	1.13e-03	1.12e-03	1.10e-03	1.10e-03	1.09e-03
STDEV										
2.17e-23	6.92e-37	1.01e-27	1.06e-37	9.90e-28	3.76e-39	8.98e-32	3.96e-41	1.32e-33	0.00e00	1.00e-33
Standard Error										
2.17e-25	6.92e-39	1.01e-29	1.06e-39	9.90e-30	3.76e-41	8.98e-34	3.96e-43	1.32e-35	0.00e00	1.00e-35
2.17e-27	6.92e-41	1.01e-31	1.06e-41	9.90e-32	3.76e-43	8.98e-36	3.96e-45	1.32e-37	0.00e00	1.00e-37
Total / Overall Standard Error										
2.168e-25										
Total Standard Deviation										
7.190e-24										
Total Signal / Noise Ratio										
3.130e12										
SE / NE										
100	100	100	100	100	100	100	100	100	#	100

The results obtained are proportional to each other and are shown in Figure **24**, where the ratio at the equation 12 condition and the result at the equilibrium result are superimposed on one of the strain values when the plane strain results are processed.

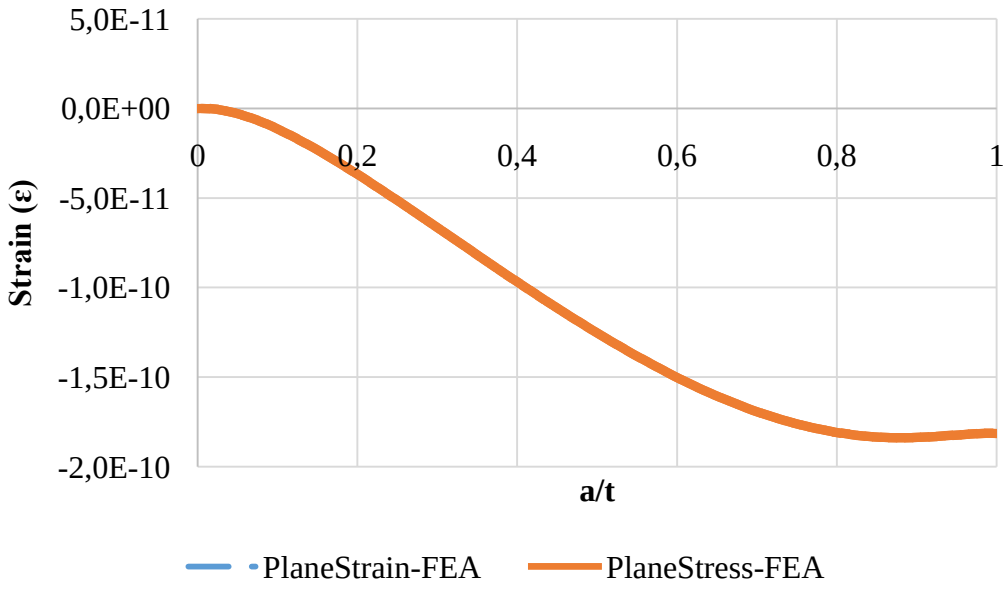

Figure 24: Proportional ratio of plane strain vs stress results.

The graph placed in Figure 23, plane strain and plane stress distributions are compared with each other independently of the elastic and poison ratio properties of the material. As expected, the difference between the two finite element approximation methods was found to be related to the poison ratio and the applied initial stress aspect.

Scaling of compliance matrix

The geometry is defined in a general form at the stage of obtaining the compliance matrix by the FEM. The reason for this is that the Legendre polynomials have a balanced distribution between [-1,1] points. The plate thickness is defined between these points and a generic compliance matrix specific to geometry is obtained for the calculation of residual stresses. In general, the compliance matrix can be scaled for the desired thickness.

The Legendre polynomials, which exhibit a balanced distribution over the point interval above, are chosen to represent the residual stress profile. Of course, every Legendre polynomial order may not show a balanced distribution. Therefore, in some Legendre order solutions, residual stresses may not be homogeneous along the cross section of the end element analysis. The unit of compliance matrixes obtained as a result of FEA can be defined as a universal consent matrix. The reason is that these values can be transformed into desired geometric dimensions by a few mathematical operations. For this, it is necessary to calculate the dimensional proportions between the dimensions of the sample and the model of the end elements in which the necessary conversion tests are to be performed. Based on this dimensional ratio, Legendre polynomials can then be transformed with the help of MatLAB. Here, using the symbolic mathematical toll of the MatLAB program, residual stress distributions can be constructed in the FEM so that the Legendre polynomials represent proportionally the same geometry. These steps can be easily accomplished with the MatLAB equations and instructions given in below Appendix-1. Subsequently, in order to obtain the compliance matrix, functions of the initial stress definition phase must be revised with MatLAB-derived polynomials to re-run the analyzes and obtain the required compliance matrix.

With the above transformation functions, the adaptation of Legendre polynomials is performed according to the sample thickness of the experiments to strain generate using the slitting method. Thus, the compliance matrix is obtained by applying the cutting process again with the model prepared in the compliance matrix FE software to be used in the residual stress calculations.

The Compliance Matrix is included in the appendix section in this thesis study, which is generated by 2 to 12 orders of Legendre polynomials with the help of the FE cutting analysis. The Legendre polynomials plot are shown in Figure.25-28.

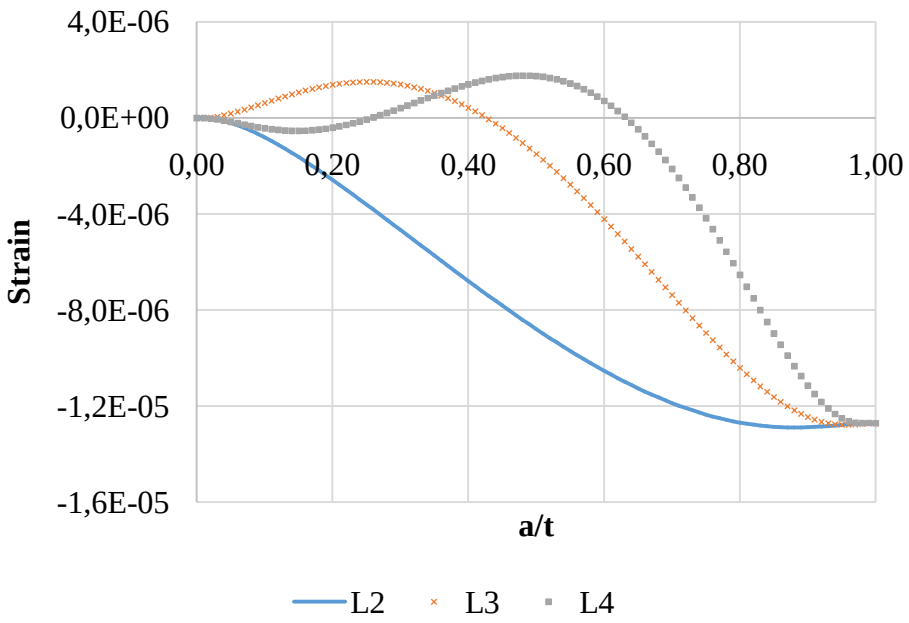

Figure 25: Compliance matrix plot Legendre (L2-4).

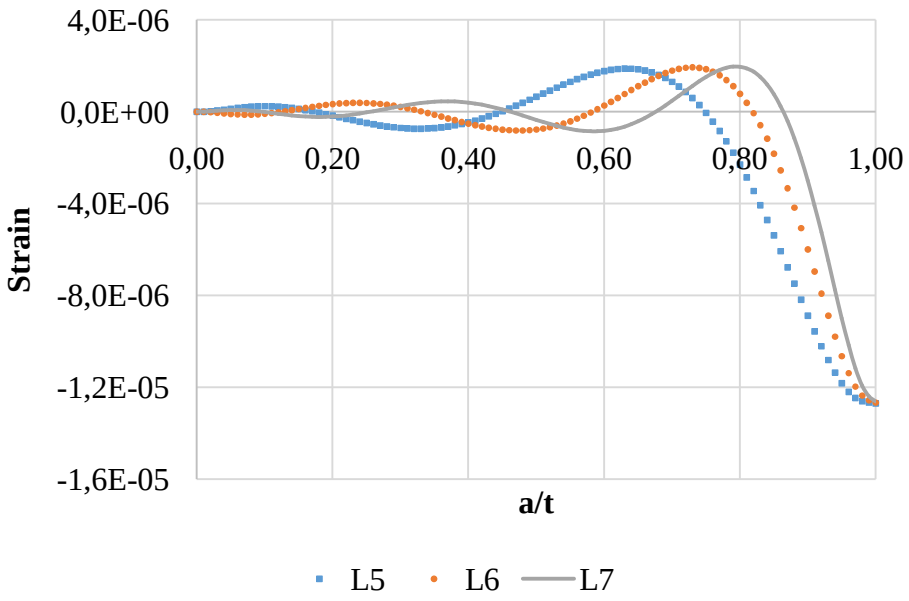

Figure 26: Compliance matrix plot Legendre (L5-7).

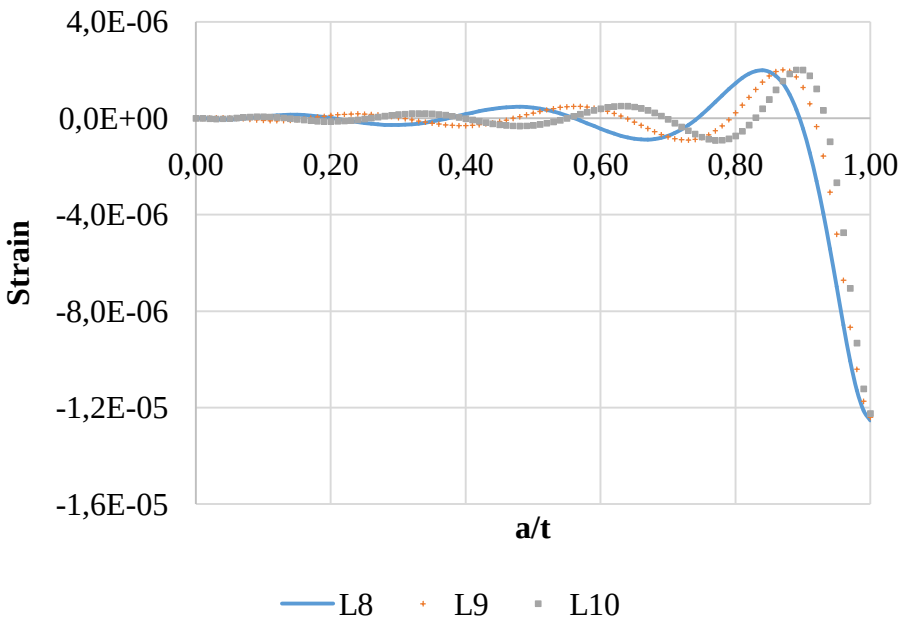

Figure 27: Compliance matrix plot Legendre (L8-10).

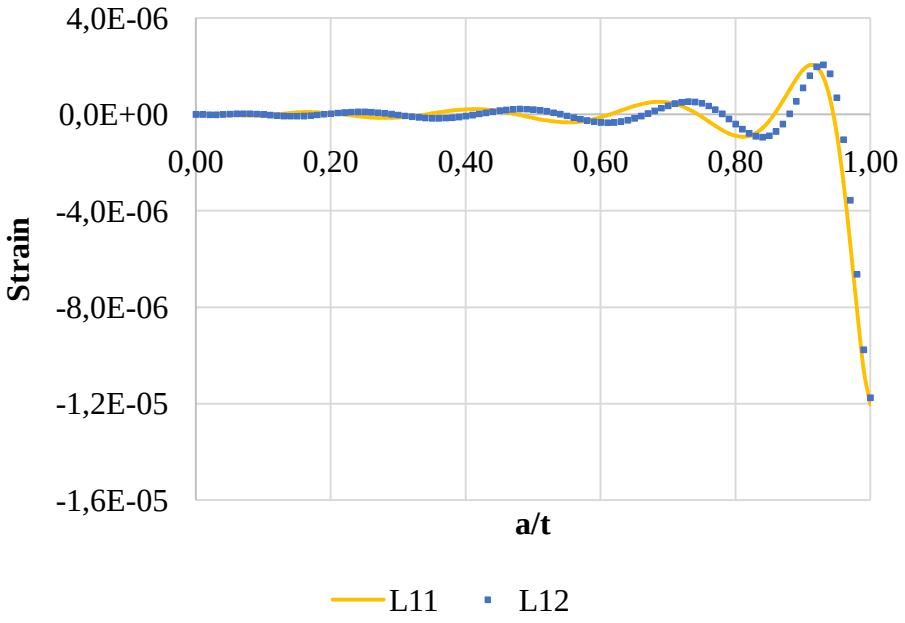

Figure 28: Compliance matrix plot Legendre (L11-12)

CHAPTER 5

APPLICATION TO COLD ROLLED ALUMINUM PLATES

Cold rolling of aluminum plate basically is carried out at room temperature for higher strength, hardness and good surface quality. In addition to this, the process needs high energy due to the higher strength of the aluminum plate at room temperature and the anisotropic properties effect [28]. In addition, the percentages of elements for the chemical composition of the AA 5083 alloy in the literature are indicated in Table 7 [73]. Aluminum 5083 also retains exceptional strength after welding. It has the highest strength of the non-heat treatable alloys but it is used for temperatures in excess of 65°C. Due to its average workability of cold forming, poor fabrication response for machinability, average weldability with gas and excellent weldability with arc and resistance welding properties in the in the production processes, AA 5083 is used in shipbuilding, rail cars, vehicle bodies, tip truck bodies, mine skips and cages, pressure vessels.

Table 7: Chemical composition for aluminum alloy 5083 [24]

Mn	Fe	Cu	Mg	Si	Zn	Ti	Cr	Al
0.4-1.0	0.4	0.1	4.0-4.9	0.4	0.25	0.15	0.05-0.25	Balanced

In addition to the chemical composition of the material in the literature, the results of spectral analysis tested in laboratories are given Table 8 in detail.

Table 8: Weight percent of spectral analysis results

Si	0.191	B	0.0063	Mo	0.013
Fe	0.290	Ba	<0.001	Na	0.0025
Cu	0.03	Be	0.00092	P	<0.002
Mn	0.528	Bi	0.011	Pb	0.0063
Mg	5.436	Ca	0.00095	Sn	0.0061
Cr	0.106	Cd	0.00077	Sr	<0.0010
Ni	<0.002	Co	0.0029	V	0.018
Zn	0.110	Ga	0.0097	Zr	<0.002
Ti	0.029	In	<0.002	Sb	<0.007
Ag	<0.0005	Li	<0.00002	Hg	0.044
Al	93.14				

As it is mentioned in previous chapters, there is a planar slit in the slitting step by step of a material containing residual stresses in increasing depth steps. The deformation near the slit will be used as a function of increasing the slit depth

resulting from the displacement of the residual stresses on the slit surface and to determine the residual stress normally normal to the slit plane before cutting. In the thickness over the samples taken from the plate is determined by the strain gage from the back and front face measured strains of the block. In typical applications in metallic materials, the slit is cut using a wire-EDM machine [19]. The strain thus released is measured by the strain gage. In the calculation of residual stresses, it is calculated according to the strain distribution, which is called the adaptation matrix determined by the analysis of the FE and measured by means of a linear system either the described matrix in the previous section.

In the cold rolling process in which the residual stress profile is to be investigated using the slitting method, which passes the metal through the rolls at temperatures below the recrystallization temperatures as at the room or ambient temperature. This process increases the yield strength and hardness of the metal. This is done by introducing defects into the crystal structure of the metal creating a hardened microstructure which prevents further slip. Because the metal is at room temperature, it is less malleable than metal above its recrystallization temperature. The cold rolling process is shown basically in Figure 1. This makes the cold rolling process a more labor-intensive and expensive process than the hot rolling process, in which the hot rolling process is excluded from the scope of this thesis.

Sample preparation for residual stress measurement by slitting method on cold rolled aluminum plate is prepared as it is shown in Figure 29. Samples with 60x100x20 mm dimensions were prepared from the related 400x400x20 mm 5083 aluminum plate. The details of the finite element analysis studies for the determination of sample sizes are explained in detail in the next section. As a result, when finding the test specimen dimensions, it is possible to reach the dimensions that will have minimum residual stress relaxation at the end of the sample cutting from the plate. The samples were removed from the plate by cutting them on the wire-EDM device. The dimensions of the determined sample are shown in Figure 29. Here, samples from 1 to 5 have prepared the residual stress measurements using the slitting method and the ring-core method with shown in capital letters. All the dimensions were measured by the help of CMM device of the sample. The sample measurement point s and planes are showed in the Figure 32 as a measurement point cloud. Experiments were carried out on series B from the samples.

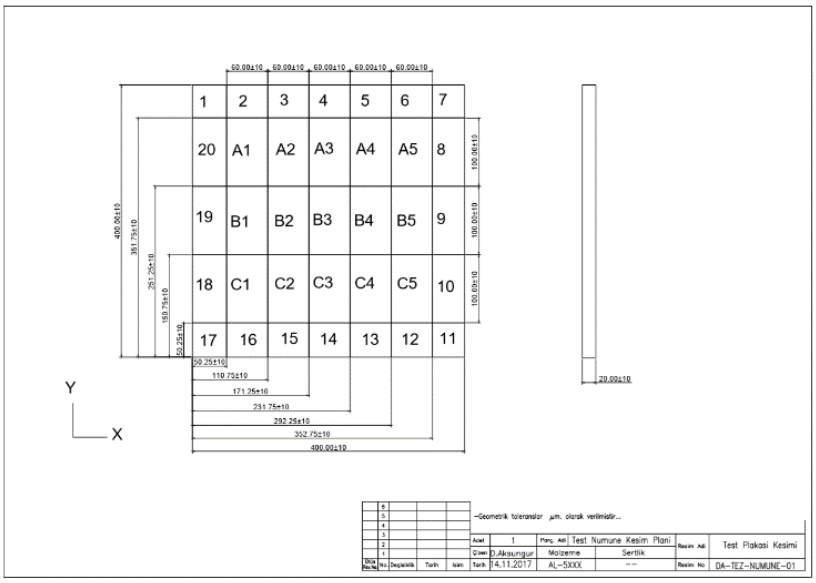

Figure 29: AA 5083 plate cutting strategy.

Measurements were taken from the CMM instrument samples to determine their dimensional size after the samples were cut. After placing the samples located according to Figure 30, the planes mentioned in Figure 31are measured as point cloud.

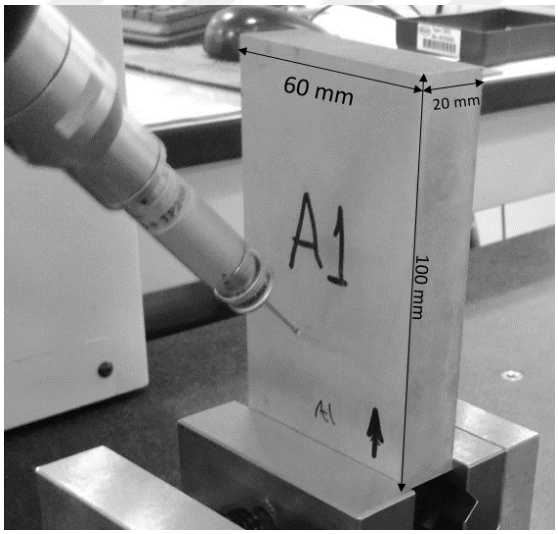

Figure 31: CMM scanning

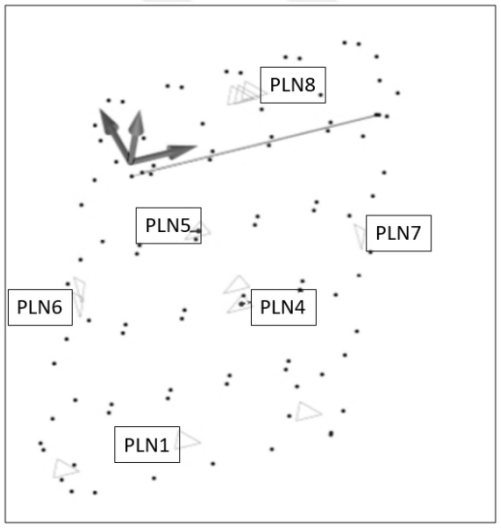

Figure 30: CMM scanning point cloud

For slitting, an apparatus design was made to hold the sample according to the size sample decided by the analysis of the FE and the cutting operation. The CAD model for positioning on the apparatus and the sample is also shown in Figure 32.

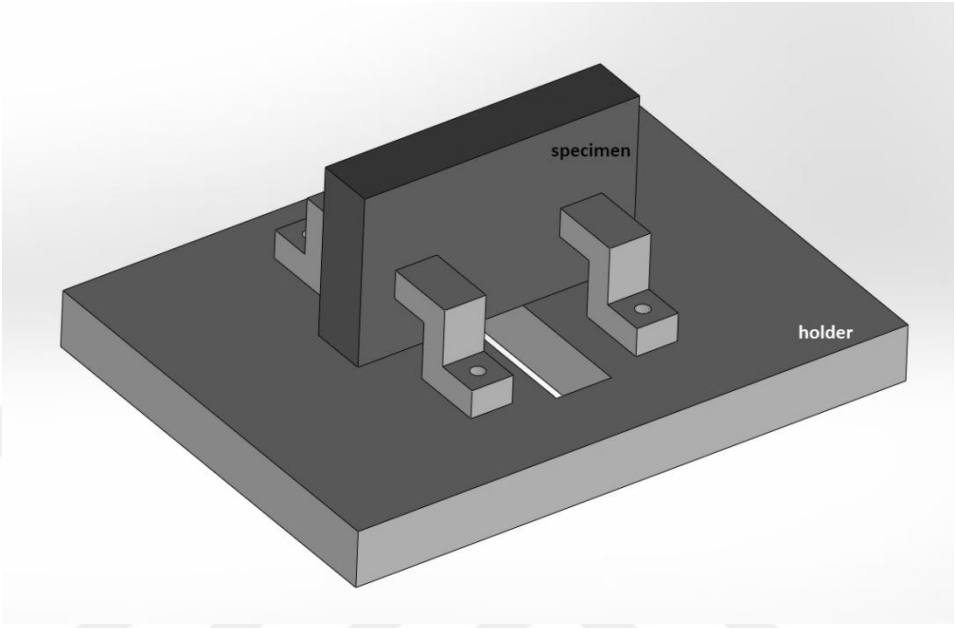

Figure 32: Specimen holder for EDM cutting.

The most important step required to perform the measurement with the Slitting method is to apply the strain gage onto the sample. A total of 2 strain gages were applied on the sample. One of them is attached to the back surface of the sample to meet the cutting line precisely. On the other hand, the front surface, which is started to cut, is bonded to the cutting line. In applications, special strain gage type C2A-62-13-062LW-350 is used for aluminum material. The strain gage length is 1.52 mm, overall length 4.45 mm, grid width 1.27 mm and overall width 2.03mm, matrix length 6.4 and width 3.56 mm respectively with cable as shown in Figure 33.

Figure 33: Example of C2A construction.

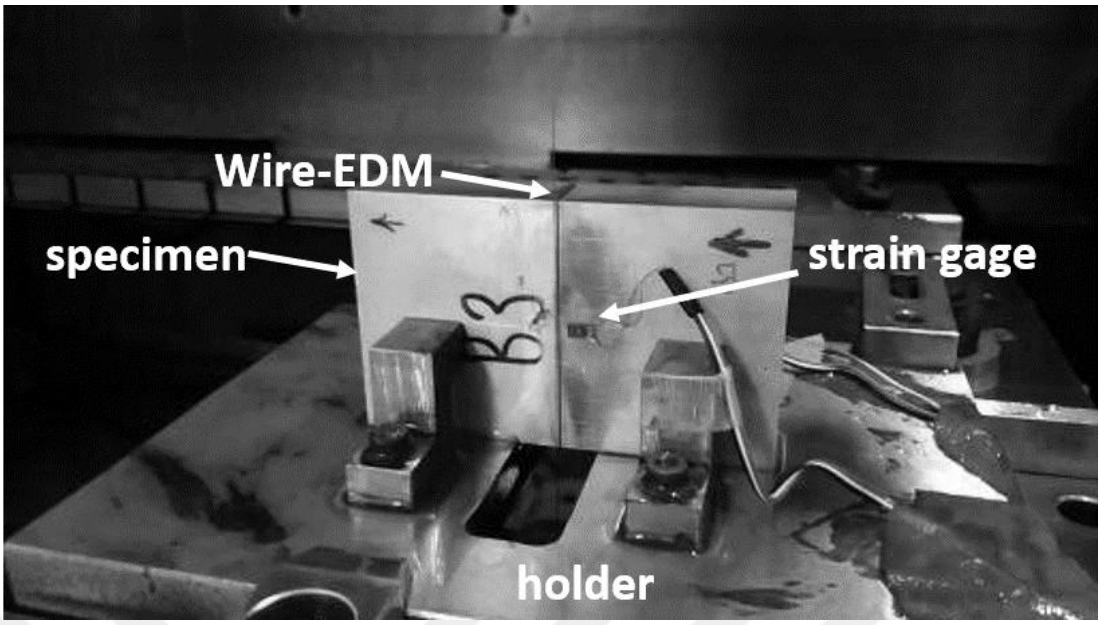

Figure 34: Specimen mounted in the EDM machine.

The holders are connected to the Sodick wire-EDM device during the execution of the tests as shown in the Figure 34. In the test, the test sample was placed between the lugs on the holder. The experiment was planned to create cuts of 18 mm with 250 micron steps and instantaneous data collection was performed at each step. Finally, at 17.75 mm, the wire EDM was broken and the cutting process was terminated. At each cutting step, the collected data was expected to be stabilized and recorded. The strain distributions in the cutting process are presented in the appendix.

As a result of literature survey, test specimen sizes were determined by using FEM. For the dimensions determined in the residual stress measurements by slitting method, it is sufficient to attach one strain gage to the backface. More than one strain gage could be applied to strengthen the measurement signal. However, in cases where the specimen width is greater than the length, residual stress measurements could be performed along the plane with multiple individual strain gage application.

Since the residual stress distribution we tried to measure was on a cold rolled thick plate, it could be measured by nondestructive methods using synchrotron or neutron diffraction methods. Approximately up to 1.5 m thickness could be measured by ND but the solution is around 1 mm^2. For these measurement nondestructive methods, a facility investment rather than a device is required. The measurement with XRD

could only be carried out by removing the material from the surface up to a range of 0.6-1 mm.

With the compliance matrix obtained in the previous section, the processing time of these collected strain data was processed by the coding performed in the MatLAB program. MatLAB codes are also presented in appendix. The inverse process is performed of the Compliance Matrix and processed with the strain data collected from the backface to find the matrix coefficients of the residual stress profile using the least square fit method.

First, the slitting method is applied and the strain results from the backface are given in Figure 35. The increase in the depth profile of the data obtained from the strain gage placed on the posterior surface was observed. This is due to the fact that the cuts formed by the EDM are approximated to the measurement area of the strain gage and the relaxation areas formed in the residual stress are due to the penetration of the strain gage into the field. The sources in the literature are likewise very small in the cuts created in the distant state to the strain gage.

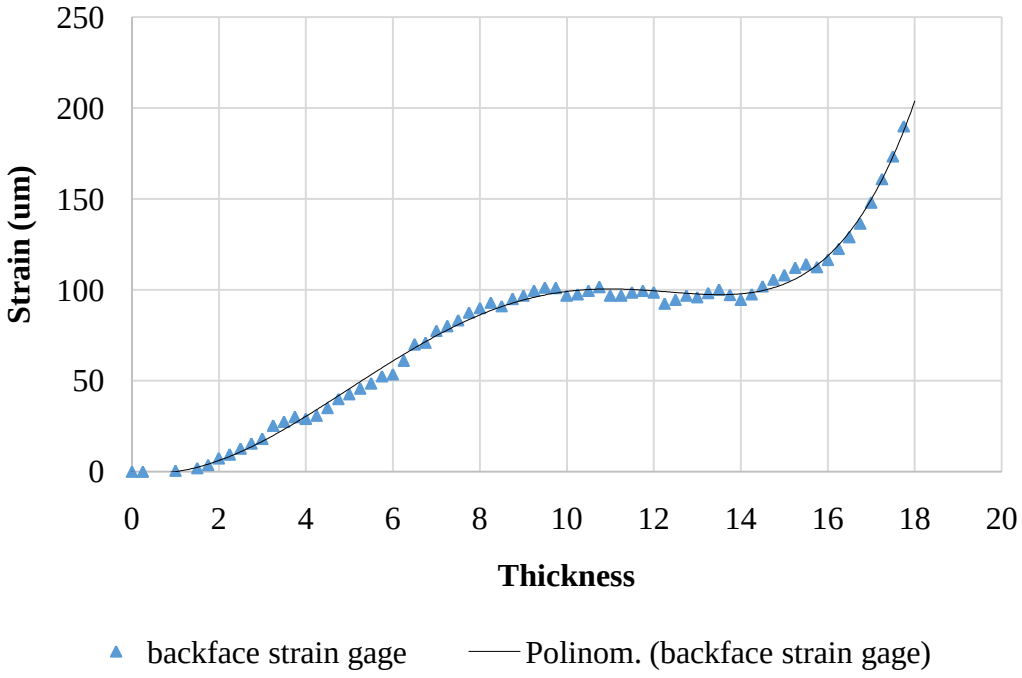

Figure 35: Slitting method strain measurement from back face strain gage

A number of mathematical operations are required to obtain the residual stresses by the slitting method after reading the strain gage data. For these operations, as already mentioned, the processes are done through the lines of code created using MatLAB

mathematical tool. As a result, the calculated results for the residual stress distribution along the section are shown in Figure 36.

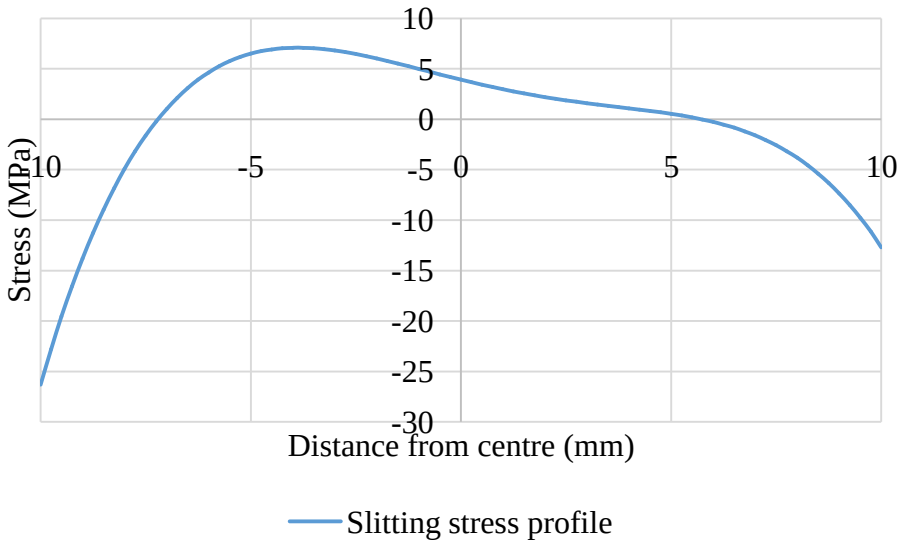

Figure 36: Slitting residual stress profile vs distance from the center.

In this study, strain data were collected and the residual stress profile in the plate was calculated. The residual stress profile obtained is similar to the overall residual stress profile in cold rolling. Instead of a direct parabolic residual stress distribution in the residual stress distribution, it is expected that there will be a decreasing trend in the center, and a similar profile has been observed in our calculations. It is noteworthy that the residual stress profile measured by the Slitting Method is asymmetric. Plates produced by cold rolling are expected to have symmetrical residual stress distribution throughout the thickness. The reason is that the profile is asymmetrical because it is thought that the plate may have passed through a flatting process or a non-homogenous heat treatment process after production.

Tests were also carried out on the specimen using the ring-core method for deeper residual stress measurements in specimens with thickness. In the tests performed, strain gage number two was stuck in parallel in the direction of the roll. The test plan is progressed with 125 micron steps up to a depth of 5 mm, and data recording is performed after approximately 30 seconds of waiting at each step. By ring-core method, rosette FRA-5-11 strain gage is used in measurements which is shown on Figure 37. The gage length is 5 mm, width 1.9mm, backing length and width is Ø12 mm and with resistance 120 ohm. The strain distributions obtained on the strain gage

numbered 2 as a result of the tests are shown in Figure 38 through the cold rolling direction as shown in Figure 38.

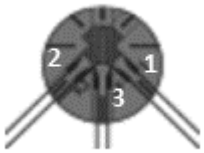

Figure 37: Ring core rosette strain gage.

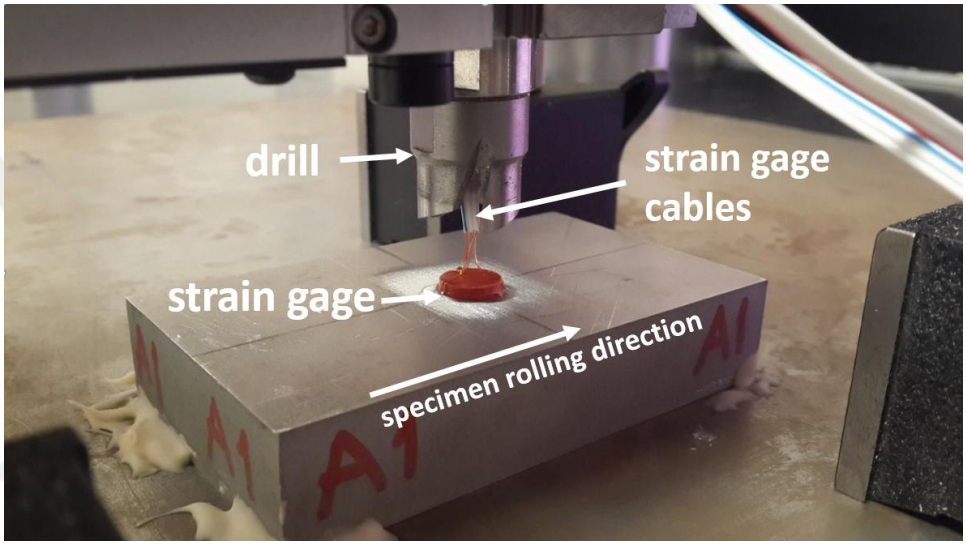

Figure 38: Ring core test setup

Here, slitting experiments were carried out and the results compared with the values read on the front surface bonded strain gage. When the figure is lowered, it can be observed that the strain values go parallel to a certain depth profile. As factors affecting here, sanding is performed with the principle of surface preparation in ring-core method. which removes the layer from the surface and is thought to cause small shifts in comparison references. In addition, in the slitting method, the strain gage adhered to the top surface is aligned so that it starts to stick at a distance of 2 mm from the cutting line. The strain gage grid center is also located away from the approx. 5 mm cutting line. Therefore, it is physically natural to observe such differences in the comparison of the measurements because of the differences in location of the strain agglomerations depending on the method.

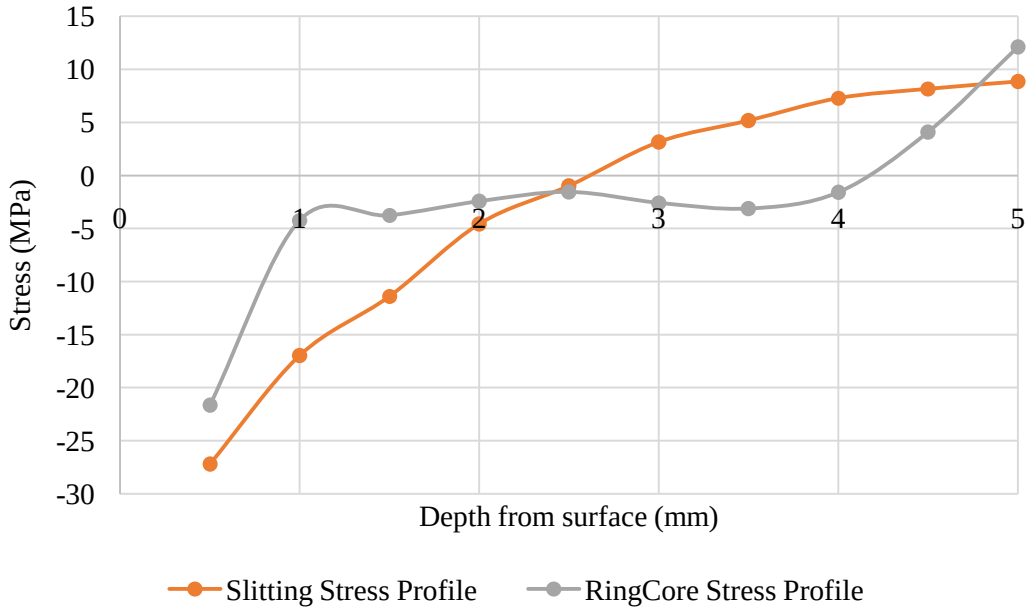

Figure 39: Slitting vs ring core residual stress measurement comparison

Although the residual stress measurements performed with two different methods and approached are not expected to give the same results, it is expected that the trends they have shown would differ in Figure 39. As a result, compression and tensile stress distributions at equivalent depths were measured for the residual stress values measured throughout the depth. Measured values can also be said to be within an error band that can be valued as close values.

When measuring with the ring core method, the strain gage no. 2 is positioned parallel to the rolling direction shown in Figure 40. The strain gage no.1 measured the residual stress in transverse direction perpendicular to the direction of rolling shown in Figure 41.

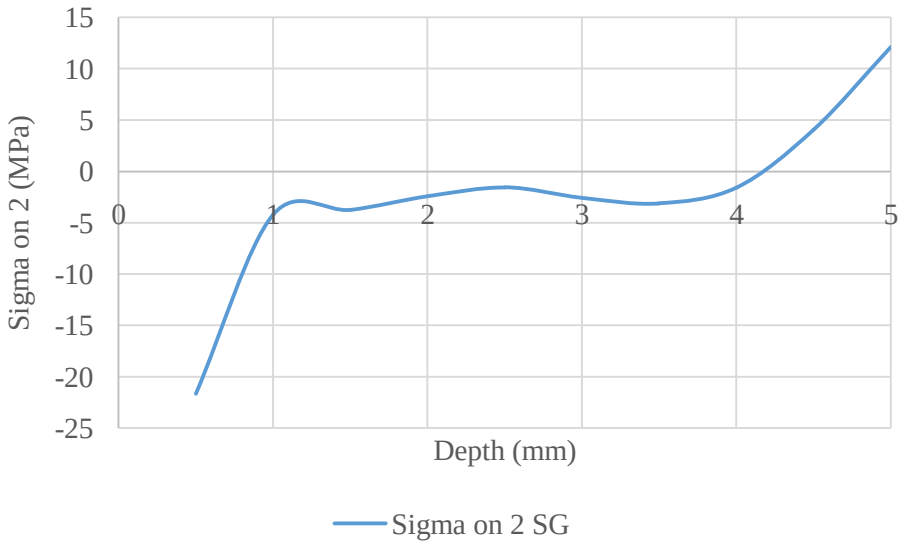

Figure 40: Ring core stress measurement through the cold rolling direction

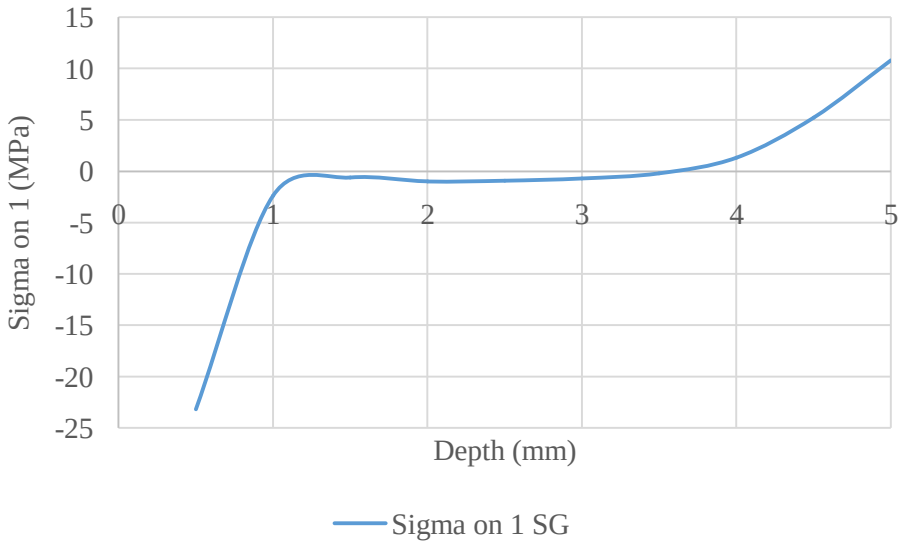

Figure 41: Ring core stress measurement through the transverse direction

CHAPTER 6

CONCLUSION

In order to perform residual stress measurements with slitting method this thesis study, compliance matrix is needed. In this context, model is prepared using finite elements in order to carry out advanced solutions for plate sample. The finite element model, both the optimum number of elements required for model optimization and the length of the sample were analyzed. As a result of these analyzes, the number of elements to be used in the plate section has been determined successfully and the sample size has been determined successfully in order to remove the samples and cause minimum stress relaxation. As a result, the samples were cut in the wire-EDM device as described in Figure 34 above for use in different tests from the AA 5083 material with dimensions of 400x400x20 mm.

As a result of finite element analysis, the strain measurements were taken from the point where the planned to take measurements by placing at the back face of the specimen and Compliance Matrix was successfully formed. A matrix coefficient to be used in the calculation of residual stress were calculated by performing numerical operations. Together with these coefficients, AA 5083 was evaluated with Legendre polynomials to calculate residual stress profile along the section. As a result of the evaluations, a similar profile distribution with cold rolling residual stress stresses was successfully observed.

In the finite element method for forward solutions, the plane strain approach has been chosen for defining cutting problem of the plate. In addition to this approach, the same model was modeled by using the plane stress approach. The main aim is to control the accuracy of the model with two approaches and to be able to create compliance matrix with the plane stress. In line with the modeling and analysis studies performed, compliance matrix was successfully established for both plane strain and plane stress solution methods. Due to the difference between the two solution methods, the calculation of the relationship between the strain values taken from the measurement point was made according to the indicators in the literature and the literature was successfully matched.

In the experimental phase, an apparatus design was performed to provide the boundary conditions in the finite element model. In the experiments, the sample is placed in this apparatus and the cutting operations are performed. Before the cutting process, strain gage applications were performed on the back and front surfaces of the specimen to be taken. In strain gage application, care was taken to align the center of the posterior surface with the strain gage grid center. The front strain gage was placed at a distance of 2 mm from the cutting line. In addition, the center line parallel to the strain gage grid is precisely centered. In these bonding steps, standard strain gage bonding procedures were followed and the adhesion lines were marked with precision marking.

HBM Quantum X, 4 channel data acquisition device was used during slitting cutting operations. With the data collection device's software CATMAN, the data were monitored instantly. The HBM Quantum X used requires an additional socket for the quarter bridge connection in the data acquisition device. A 3-wire strain gauge can be installed on the socket. At this point, the connection of the cables is important. At this stage, since up-to-date software should be used in our initial experiments, system errors could not be detected in connection errors and similar signal problems. After this stage, data collection system and software updates were carried out and experiments continued. These experiences gained in the first experiments caused a loss of time.

The cutting was carried out in the wire-EDM in steps of 250 microns. After each progress, a certain period of time was waited and strain readings were successfully recorded. During the cutting process, the wire breakage problem was not encountered up to 17,750 mm. It has been successfully completed in progress to this depth.

In the follow-up of the test procedure, the numerical side of the residual stress calculations was performed by a program written in the MatLAB. Compliance Matrix which is formed by strain reading in the finite element program, has reached the coefficients mentioned above matrix A_j.

Samples were also removed from the plate for the ring-core residual stress measurement method. In this process, FRA rosette type 120-ohm strain gage is used. A number of problems were encountered during the experiments with this device. In the experiments on cold rolled AA material, drill bit jamming and drill breakage

problems were encountered. Due to the fact that the aluminum material is not magnetic, the magnet cannot be used for the removal of the chips during drilling. The chip removal process continued during the perforations with the help of the wooden rods to collect the chips around the hole. At the same time, the lubricant has been used in certain progression steps to reduce friction on the contact surfaces between the drill bit and the AA material. Experience of such experiments during the experiments was successfully continued to the test procedure to a depth of 5 mm. For this experiment, the SINT Ring-Core measuring device was used.

A more accurate approach is to compare the strain gage data placed on the surface, which is placed parallel to the rolling direction. At the same time, the ring gauge measurements were compared with the strain gage along to the rolling direction. This was observed to be parallel between the strain data from the front surface to a certain depth.

As a result, the unit for measuring the residual stress by slitting method has been formed successfully by using finite element method from advanced solution methods. Experimental design and signal collection issues must be carried out in a precise way. Experimental matrix should be removed, especially by providing the boundary conditions in the finite element model. Calculation of the residual stress profile through the thickness by using the slitting method on cold rolled plate with numerical operations and the results of the calculation has been completed successfully.

FUTURE WORKS

In line with the studies carried out in the future, the list for the works that are planned to be done in the future.

1. AA 5083 material has been commercially supplied to the research center where the tests and studies will be carried out. For this reason, the manufacturing history of the operations could not be known on the material before coming to the research center. Some stress relief operations may have been performed on the material within the possibilities. Therefore, the implementation of this method on direct cold rolled material will ensure that the results are more reliable. At this stage, it is necessary to work with a cold rolling manufacturer.

2. When the literature is examined, it is observed that the areas cutting with wire-EDM is undergoing plastic deformation. This effect must be taken into account because it affects the residual stress measurement. In this thesis, the effects of local plastic deformations were not investigated. Therefore, plastic effects and the effects of residual stress measurement should be evaluated in the progress of the study.

REFERENCES:

[1] M. J. Lee and M. R. Hill, "Effect of Strain Gage Length When Determining Residual Stress by Slitting," *J. Eng. Mater. Technol.*, vol. 129, no. 1, p. 143, 2007.

[2] M. B. Prime, "Residual stress measurement by successive extension of a slot: the crack compliance metod," *Appl. Mech. Rev.*, vol. 836, 1999.

[3] G. S. Schajer and Y. An, "Residual stress determination using cross-slitting and dual-axis ESPI," *Proc. Soc. Exp. Mech. Inc.*, vol. 67, pp. 169–177, 2010.

[4] G. Montay, O. Sicot, A. Maras, E. Rouhaud, and M. François, "Two dimensions residual stresses analysis through incremental groove machining combined with electronic speckle pattern interferometry," *Exp. Mech.*, vol. 49, no. 4, pp. 459–469, 2009.

[5] and R. G. Lu J, James M, *Handbook of Measurement of Residual Stress*. 1996.

[6] G. S. Schajer, "Residual Stresses: Measurement by Destructive methods.," *Buschow, K. H. J. al. (eds)Encyclopedia Matrials Sciemce Technol.*, vol. Section 5a, no. Elsevier Science, Oxford, 2001.

[7] G. S. Schajer, "Relaxation Methods for Measuring Residual Stresses: Techniques and Opportunities," *Exp. Mech.*, vol. 50, no. 8, pp. 1117–1127, 2010.

[8] G. S. Schajer, *Practical Residual Stress Measurement Methods*. 2013.

[9] H. W. Walton, "Deflection Methods to Estimate Residual Stress," *Handb. Residual Stress Deform. Steel. ASM Int. Matrerials Park. OH*, vol. 89–98, 2002.

[10] A. S. for T. and Materials, *ASTM Standard Practice for Estimating the Approximate Residual Circumferential Stress in Straight Thin-walled Tubing. Standard test method E1928-07*. 2007.

[11] W. T. Treuting, R. G., Read, "A Mechanical Determination of Biaxial Residual Stress in Sheet Materials," *J. Appl. Phys.*, vol. 22, no. 2, pp. 130–134, 1951.

[12] G. Sachs, G., Espey, "The Measurement of Residual Stresses in Metal.," *Iron Age.*, vol. Sept, no. 18, pp. 63–71, 1941.

[13] A. S. for T. and Materials, *ASTM Standard Test Method for Determining Residual Stresses by the Hole-Drilling Strain-Gage Method, Standard Test Method E837-08*. 2008.

[14] P. S. Grant, P. V., Lord, J. D., Whitehead, "The Measurement of Residual Stresses by the Incremental Hole Drilling Technique," *Meas. Good Pract. Guid.*, vol. 53, no. National Physical Laboratory, UK., 2002.

[15] M. Group, "Measurement of Residual Stresses by Hole-Drilling Strain Gage Method.," *Vishay Meas. Group, Raleigh, NC*, vol. Tech Note, 2001.

[16] S. Kiel, “Experimental Determination of Residual Stresses with the Ring-Core Method and an On-Line Measuring System.,” *Exp. Tech.*, vol. 16, no. 5, pp. 17–24, 1922.

[17] B. Ajovalasit, A., Petrucci, G., Zuccarello, “Determination of Non-Uniform Residual Stresses using the Ring-Core Method,” *J. Eng. Mater. Technol.*, vol. 118, no. 2, pp. 224–228, 1996.

[18] and F. F. Leggatt RH, Smith DJ, Smith SD, “Development and Experimental Validation of the Deep Hole Method for Residual Stress Measurement,” *J Strain Anal Eng Des*, vol. 31, no. 3, pp. 177–186, 1996.

[19] M. R. DeWald, A. T., Hill, “Improved Data Reduction for the Deep-Hole Method of Residual Stress Measurement,” *J. Strain Anal.*, vol. 38, no. 1, pp. 65–78, 2003.

[20] M. B. Prime, “Cross-Sectional Mapping of Residual Stresses by Measuring the Surface Contour After a Cut.,” *J. Eng. Mater. Technol.*, vol. 123, no. 2, pp. 162–168, 2001.

[21] M. R. DeWald, A. T., Hill, “Multi-Axial Contour Method for Mapping Residual Stresses in Continuously Processed Bodies.,” *Exp. Mech.*, vol. 46, no. 4, pp. 473–490, 2006.

[22] P. J. Kelleher, J., Prime, M. B., Buttle, D., Mummery, P. M., Webster, P. J., Shackleton, J., Withers, “The Measurement of Residual Stress in Railway Rails by Diffraction and other Methods,” *J. Neutron Res.*, vol. 11, no. 4, pp. 187–193, 2003.

[23] SAE, “Residual Stress Measurement by X-ray Diffraction.,” *SAE J784, Soc. Automot. Eng. Handb. Suppl. Warrendale, PA.*, 2003.

[24] T. Reimers, W., Pyzalla, A., Broda, M., Brusch, G., Dantz, D., Schmackers, T., Liss, K-D., Tschentscher, “The Use of High-Energy Synchrotron Diffraction for Residual Stress Analyses.,” *J. Mater. Sci. Lett.*, vol. 18, no. 7, pp. 581–583, 1999.

[25] Y. Hayaski, M., Ohkido, S., Minakawa, N., and Murii, “Residual Stress Distribution Measurement in Plastically Bent Carbon Steel by Neutron Diffraction,” *5th Int. Conf. Residual Stress. Link¨oping Univ. Sweden,* vol. 2, pp. 762–769, 1997.

[26] T. M. Root, J. H., Hosbaus, R. R., Holden, “‘Neutron Diffraction Measurements of Residual Stresses Near a Pin Hole in a Solid-Fuel Booster Rocket Casing,” *Pract. Appl. Residual Stress Technol. ASM Int.*, pp. 83–93, 1991.

[27] H. Watanabe, H. Honjo, and K. Miyasaka, “Selection of Work Roll Diameter for Cold Rolling Mill,” *Trans. ISIJ*, vol. 23, pp. 21–30, 1983.

[28] S. Kalpakjian, S. R. Schmid, and H. Musa, “Manufacturing Engineering and Technology,” *Manuf. Eng. Technol.*, vol. 6, p. 1197, 2009.

[29] S. Vaidyanathan and I. Finnie, “Determination of Residual Stresses From Stress Intensity Factor Measurements,” *J. Basic Eng.*, vol. 93, no. 2, pp. 242–246, 1971.

[30] W. Finnie, I., Cheng, “A Summary of Past Contributions on Residual Stresses,” *Mater. Sci. Forum*, no. 404–407, pp. 509–514, 2002.

[31] W. Finnie, I., Cheng, “Residual stress measurement by the introduction of slots or cracks, Localized Damage IV Computer Aided Assessment and Control of Localized Damage,” *Comput. Mech. Inc., Billerica, MA, USA*, pp. 37–51, 1996.

[32] W. Cheng and I. Finnie, “A method for measurement of axisymmetric axial residual stresses in circumferentially welded thin-walled cylinders,” *J. Eng. Mater. Technol.*, vol. 107, no. 3, pp. 181–185, 1985.

[33] W. Cheng, I. Finnie, and O. Vardar, “Measurement of Residual Stresses Near the Surface Using the Crack Compliance Method,” *J. Eng. Mater. Technol.*, vol. 113, no. 2, p. 199, 1991.

[34] I. Cheng, W., Finnie, “Residual Stress Measurement and the Slitting Method,” *Springer New York.*, 2007.

[35] M. J. Lee and M. R. Hill, “Intralaboratory repeatability of residual stress determined by the slitting method,” *Exp. Mech.*, vol. 47, no. 6, pp. 745–752, 2007.

[36] M. B. Prime, “The Slitting (Crack Compliance) Method for Measuring Residual Stress,” 2012. .

[37] A.] Aydiner, C. C., Ustundag, E., Prime, M. B., Peker, “Modeling and Measurement of Residual Stresses in a Bulk Metallic Glass Plate,” *J. Non-Crystalline Solids*, vol. 316, no. 1, pp. 82–95, 2003.

[38] G. F. Midha, P. S., Modlen, “Residual Stress Relief in Cold-extruded Rod,” *Met. Technol.*, vol. 3, no. 11, pp. 529–533, 1976.

[39] M. R. Rankin, J. E., Hill, “Measurement of Thickness-average Residual Stress Near the Edge of a Thin Laser Peened Strip,” *J. Eng. Mater. Technol.*, vol. 125, no. 3, pp. 283–293, 2003.

[40] M. B. Prime and M. R. Hill, “Residual stress, stress relief and inhomogeneity in Al plate,” *Scr. Mater.*, vol. 46, pp. 77–82, 2002.

[41] M. B. Prime *et al.*, “Residual Stress Measurement and Prediction In a Hardened Steel Ring,” *Mater. Sci. Forum*, vol. 836, pp. 347–349, 2000.

[42] M. R. Hill and W.-Y. Lin, “Residual Stress Measurement in a Ceramic-Metallic Graded Material,” *J. Eng. Mater. Technol.*, vol. 124, no. 2, p. 185, 2002.

[43] K. I.] DeWald, A. T., Rankin, J. E., Hill, M. R., Schaffers, “An Improved Cutting Plan for Removing Laser Amplifier Slabs from Yb:S-FAP Single Crystals Using Residual Stress Measurement and Finite Element Modeling,” *J. Cryst. Growth*, vol. 265, no. 3–4, pp. 627–641, 2004.

[44] W. A. Taylor, D. J., Watkins, T. R., Hubbard, C. R., Hill, M. R., Meith, “Residual Stress Measurements of Explosively Clad Cylindrical Pressure Vessels,” *J. Press. Vessel Technol.*, vol. 134, no. 2, p. 11501, 2012.

[45] W. Cheng, I. Finnie, M. Gremaud, and M. B. Prime, “Measurement of Near

Surface Residual Stresses Using Electric Discharge Wire Machining," *J. Eng. Mater. Technol.*, vol. 116, no. 1, p. 1, 1994.

[46] L. A. Rankin, J. E., Hill, M. R., Hackel, "The Effects of Process Variations on Residual Stress in Laser Peened 7049 T73 Aluminum Alloy," *Mater. Sci. Eng.*, vol. 349, no. 1–2, pp. 279–291, 2003.

[47] M. R. Makino, A., Nelson, D. V., Hill, "Hole-within-a-hole Method for Determining Residual Stresses," *J. Eng. Mater. Technol.*, vol. 133, no. 21020, 2011.

[48] W. Cheng and I. Finnie, "Deformation of an edge-cracked strip subjected to an arbitrary shear surface traction on the crack faces," *Eng. Fract. Mech.*, vol. 43, no. 1, pp. 33–39, 1992.

[49] I. Cheng, W., and Finnie, "The crack compliance method for residual stress management," *Weld. World*, vol. 28, no. 516, pp. 103–110, 1990.

[50] A. E. Albert, "Regression and the Moore-Penrose Pseudoinverse," *Acad. Press*, 1972.

[51] B. HF, "The Propagation of Cracks and the Energy of Elastic Deformation," *Trans Amer Soc Mech Eng*, vol. 80, pp. 1225–1230, 1958.

[52] M. Perl and R. Arone, "An Axisymmetric Stress Release Method for Measuring the Autofrettage Level in Thick-Walled Cylinders — Part I : Basic Concept and Numerical Simulation," vol. 116, no. November 1994, pp. 384–388, 2016.

[53] - Fett T and Munz D, "Stress Intensity Factors and Weight Functions," *Comput. Mech. Publ. Southampton,UK*, vol. 76, 1997.

[54] W. X. and C. AJ, "Weight Functions and Stress Intensity Factor Solutions," *Pergamon Press. Engl.*, 1991.

[55] Y. N. and T. Takaai, "X－ray Measurement of Distribution of Residual Stress in Cold Rolled 5083Aluminum Alloy," *J. Japan Inst. Met.*, vol. 56, no. 11, pp. 1289–1295, 1992.

[56] H. J. Schindler and P. Bertschinger, "Some steps towards automation of the crack compliance method to measure residual stress distributions," *Proc. 5th Int. Conf. Res. Stress. ICRS-5, eds. Ericsson, T., Oden, M. Andersson, A, Linkoping, Sweden*, vol. 1, no. January 1997, 1997.

[57] H. J. Schindler, W. Cheng, and I. Finnie, "Experimental determination of stress intensity factors due to residual stresses," *Exp. Mech.*, vol. 37, no. 3, pp. 272–277, 1997.

[58] M. B. Prime, "Plasticity effects in incremental slitting measurement of residual stresses," *Eng. Fract. Mech.*, vol. 77, no. 10, pp. 1552–1566, 2010.

[59] B. Winiarski, R. M. Langford, J. Tian, Y. Yokoyama, P. K. Liaw, and P. J. Withers, "Mapping residual stress distributions at the micron scale in amorphous materials," *Metall. Mater. Trans. A Phys. Metall. Mater. Sci.*, vol. 41, no. 7, pp. 1743–1751, 2010.

[60] M. B. Prime and M. L. Steinzig, “Beyond the Streetlight Effect: A United Future for Relaxation and Diffraction Methods for Residual Stress Measurement,” *9th Eur. Conf. Residual Stress.*, vol. 996, no. August, pp. 234–242, 2014.

[61] E. Procedure, F. O. R. Crack, and R. Stress, “Experimental Procedure For Crack Compliance (Slitting) Measurement Of Residual Stress,” vol. 836, pp. 0–6.

[62] K. Ueda, Y. and Fukuda, “New measuring method of three dimensional welding residual stresses based on newly proposed principle of inherent strain,” *Nav. Archit. Eng.*, vol. 18, no. 146163, 1980.

[63] G. S. Schajer and M. B. Prime, “Residual Stress Solution Extrapolation for the Slitting Method Using Equilibrium Constraints,” *J. Eng. Mater. Technol.*, vol. 129, no. 2, p. 227, 2007.

[64] M. Gremaud, W. Cheng, I. Finnie, and M. B. Prime, “The Compliance Method For Measurement Of Near-Surface Residual-Stresses - Analytical Background,” vol. 116, no. October 1994, pp. 550–555, 1994.

[65] M. Beghini and L. Bertini, “Residual stress modelling by experimental measurements and finite element analysis,” *J. Strain Anal. Eng. Des.*, vol. 25, no. 2, 1990.

[66] G. S. Schajer and M. B. Prime, “Use of Inverse Solutions for Residual Stress Measurements,” *J. Eng. Mater. Technol.*, vol. 128, no. 3, p. 375, 2006.

[67] A. Tikhonov, A., Goncharsky, A., Stepanov, V., and Yagola, “Numerical Methods for the Solution of Ill-Posed Problems,” *Kluwer, Dordrecht. Liu*, 1995.

[68] K. J. Kang and S. Y. Seol, “Measurement of Residual Stresses in a Circular Ring Using the Successive Cracking Method,” vol. 1, no. April 1996, 2017.

[69] M. T. Milan *et al.*, “Residual stress evaluation of AA2024-T3 friction stir welded joints,” *J. Mater. Eng. Perform.*, vol. 16, no. 1, pp. 86–92, 2007.

[70] K. W. Jones and M. L. Dunn, “Fatigue crack growth through a residual stress field introduced by plastic beam bending,” *Fatigue Fract. Eng. Mater. Struct.*, vol. 31, no. 10, pp. 863–875, 2008.

[71] S. Nervi, B. A. Szabo, and K. A. Young, “Prediction of Distortion of Airframe Components Made from Aluminum Plates,” *Aiaa J.*, vol. 47, no. 7, pp. 1635–1641, 2009.

[72] W. Wong and M. R. Hill, “Superposition and Destructive Residual Stress Measurements,” *Exp. Mech.*, vol. 53, no. 3, pp. 339–344, 2013.

[73] M. B. Prime and D. L. Crane, “Slitting method measurement of residual stress profiles, including stress discontinuities, in layered specimens,” *Conf. Proc. Soc. Exp. Mech. Ser.*, vol. 8, pp. 93–102, 2014.

[74] thyssenkrupp M. (UK) Ltd, “Aluminium Alloy 5083-O H111 Material Data Sheet.”

APPENDICES

APPENDIX-1

MatLAB code for slitting stress calculation.

```
clear all
%compliance matrix for Legendre 2 to 4 orders derived with FEM
C_L24;
%calculation of Aij coeff
A=(70000/(1-
0.33^2))*((inv(transpose(C_L24)*C_L24))*transpose(C_L24))*strain;
%Distance from the center
at=-10:0.25:10;
%stress calculation
stress=0;
%Legendre polinomials
for i=1:3;
P(:,i)=legendreP(i+1,-10:0.25:10);
end
%Stress calculation
for ii=1:3;
stress=stress+A(ii)*P(:,ii);
end
```

APPENDIX-2

Unit thickness conversion of Legendre polynomials with MatLAB:

```
%geometric conversion compliance matrix
% c: geometric ratio
% x: thicknes function variable

c=x/10;

% Legendre 2nd order conversion
L2=legendreP(2,c);

% Result of Legendre 2nd order conversion
L2 = (3*x^2)/200 - 1/2;

% the first and second integrals must be zero to
% provide residual stress balance.
int(L2,[-1,1])
ans = -99/100;

%for the moment balance
L22=L2*x;
L22 = x*((3*x^2)/200 - 1/2;

% Result of Legendre 2nd order moment balanced
int(L22,[-1,1])
ans = 0;
```

APPENDIX-3: 8 L - Specimen Length of Legendre Polynomials & Compliance Matrix

Inc	a	a/t	L2	L3	L4	L5	L6	L7	L8	L9	L10	L11	L12
0	0.00	0.00	0.000E+00	0.000E+00	0.000E+00	0.000E+00	0.000E+00	0.000E+00	0.000E+00	0.000E+00	0.000E+00	0.000E+00	0.000E+00
1	0.02	0.01	7.492E-13	1.807E-16	4.320E-14	4.128E-16	-1.852E-14	9.177E-16	1.366E-15	3.131E-15	1.726E-15	1.495E-14	8.117E-15
2	0.04	0.02	-1.996E-08	1.943E-08	-1.873E-08	1.788E-08	-1.689E-08	1.579E-08	-1.459E-08	1.332E-08	-1.199E-08	1.063E-08	-9.256E-09
3	0.06	0.03	-6.308E-08	5.977E-08	-5.555E-08	5.057E-08	-4.500E-08	3.903E-08	-3.286E-08	2.669E-08	-2.070E-08	1.506E-08	-9.923E-09
4	0.08	0.04	-1.259E-07	1.161E-07	-1.040E-07	9.001E-08	-7.496E-08	5.955E-08	-4.450E-08	3.045E-08	-1.793E-08	7.363E-09	1.005E-09
5	0.10	0.05	-2.060E-07	1.850E-07	-1.592E-07	1.306E-07	-1.009E-07	7.196E-08	-4.540E-08	2.254E-08	-4.271E-09	-8.958E-09	1.715E-08
6	0.12	0.06	-3.015E-07	2.632E-07	-2.176E-07	1.683E-07	-1.192E-07	7.382E-08	-3.506E-08	4.832E-09	1.599E-08	-2.756E-08	3.095E-08
7	0.14	0.07	-4.105E-07	3.484E-07	-2.759E-07	2.001E-07	-1.277E-07	6.471E-08	-1.510E-08	-1.898E-08	3.756E-08	-4.249E-08	3.701E-08
8	0.16	0.08	-5.317E-07	4.383E-07	-3.318E-07	2.240E-07	-1.258E-07	4.552E-08	1.169E-08	-4.465E-08	5.565E-08	-4.964E-08	3.311E-08
9	0.18	0.09	-6.638E-07	5.310E-07	-3.833E-07	2.387E-07	-1.133E-07	1.802E-08	4.208E-08	-6.821E-08	6.671E-08	-4.711E-08	1.988E-08
10	0.20	0.10	-8.055E-07	6.249E-07	-4.287E-07	2.436E-07	-9.105E-08	-1.554E-08	7.277E-08	-8.638E-08	6.872E-08	-3.508E-08	1.123E-11
11	0.22	0.11	-9.560E-07	7.185E-07	-4.670E-07	2.383E-07	-6.021E-08	-5.269E-08	1.008E-07	-9.685E-08	6.112E-08	-1.535E-08	-2.267E-08
12	0.24	0.12	-1.114E-06	8.107E-07	-4.972E-07	2.229E-07	-2.227E-08	-9.096E-08	1.236E-07	-9.829E-08	4.467E-08	9.225E-09	-4.411E-08
13	0.26	0.13	-1.280E-06	9.001E-07	-5.185E-07	1.980E-07	2.110E-08	-1.280E-07	1.394E-07	-9.036E-08	2.109E-08	3.530E-08	-6.072E-08
14	0.28	0.14	-1.451E-06	9.860E-07	-5.306E-07	1.642E-07	6.811E-08	-1.616E-07	1.467E-07	-7.353E-08	-7.221E-09	5.953E-08	-6.985E-08
15	0.30	0.15	-1.629E-06	1.067E-06	-5.332E-07	1.222E-07	1.170E-07	-1.900E-07	1.450E-07	-4.902E-08	-3.752E-08	7.895E-08	-7.003E-08
16	0.32	0.16	-1.811E-06	1.144E-06	-5.261E-07	7.324E-08	1.659E-07	-2.117E-07	1.342E-07	-1.855E-08	-6.700E-08	9.125E-08	-6.102E-08
17	0.34	0.17	-1.998E-06	1.214E-06	-5.094E-07	1.826E-08	2.132E-07	-2.256E-07	1.146E-07	1.583E-08	-9.304E-08	9.499E-08	-4.373E-08
18	0.36	0.18	-2.189E-06	1.278E-06	-4.831E-07	-4.155E-08	2.574E-07	-2.309E-07	8.712E-08	5.183E-08	-1.134E-07	8.957E-08	-2.000E-08
19	0.38	0.19	-2.383E-06	1.334E-06	-4.476E-07	-1.050E-07	2.969E-07	-2.272E-07	5.307E-08	8.717E-08	-1.263E-07	7.531E-08	7.654E-09
20	0.40	0.20	-2.581E-06	1.384E-06	-4.032E-07	-1.708E-07	3.307E-07	-2.144E-07	1.394E-08	1.197E-07	-1.306E-07	5.327E-08	3.638E-08
21	0.42	0.21	-2.782E-06	1.425E-06	-3.503E-07	-2.378E-07	3.576E-07	-1.928E-07	-2.855E-08	1.473E-07	-1.258E-07	2.518E-08	6.328E-08
22	0.44	0.22	-2.985E-06	1.458E-06	-2.894E-07	-3.047E-07	3.768E-07	-1.629E-07	-7.257E-08	1.684E-07	-1.120E-07	-6.801E-09	8.567E-08

23	0.46	0.23	-3.191E-06	1.483E-06	-2.209E-07	-3.704E-07	3.875E-07	-1.255E-07	-1.162E-07	1.817E-07	-8.990E-08	-4.021E-08	1.013E-07
24	0.48	0.24	-3.398E-06	1.498E-06	-1.456E-07	-4.337E-07	3.894E-07	-8.165E-08	-1.577E-07	1.862E-07	-6.065E-08	-7.251E-08	1.086E-07
25	0.50	0.25	-3.607E-06	1.505E-06	-6.390E-08	-4.935E-07	3.821E-07	-3.252E-08	-1.953E-07	1.815E-07	-2.588E-08	-1.013E-07	1.067E-07
26	0.52	0.26	-3.817E-06	1.502E-06	2.335E-08	-5.488E-07	3.656E-07	2.055E-08	-2.274E-07	1.675E-07	1.246E-08	-1.243E-07	9.549E-08
27	0.54	0.27	-4.029E-06	1.490E-06	1.155E-07	-5.986E-07	3.399E-07	7.613E-08	-2.526E-07	1.448E-07	5.224E-08	-1.399E-07	7.564E-08
28	0.56	0.28	-4.241E-06	1.468E-06	2.119E-07	-6.421E-07	3.053E-07	1.327E-07	-2.698E-07	1.139E-07	9.126E-08	-1.466E-07	4.849E-08
29	0.58	0.29	-4.454E-06	1.437E-06	3.116E-07	-6.784E-07	2.622E-07	1.888E-07	-2.782E-07	7.610E-08	1.273E-07	-1.438E-07	1.597E-08
30	0.60	0.30	-4.668E-06	1.395E-06	4.140E-07	-7.067E-07	2.113E-07	2.427E-07	-2.771E-07	3.283E-08	1.584E-07	-1.315E-07	-1.959E-08
31	0.62	0.31	-4.882E-06	1.344E-06	5.182E-07	-7.265E-07	1.533E-07	2.931E-07	-2.663E-07	-1.425E-08	1.826E-07	-1.099E-07	-5.558E-08
32	0.64	0.32	-5.096E-06	1.283E-06	6.235E-07	-7.373E-07	8.895E-08	3.386E-07	-2.457E-07	-6.326E-08	1.986E-07	-8.021E-08	-8.937E-08
33	0.66	0.33	-5.310E-06	1.211E-06	7.289E-07	-7.384E-07	1.934E-08	3.777E-07	-2.158E-07	-1.123E-07	2.051E-07	-4.393E-08	-1.184E-07
34	0.68	0.34	-5.524E-06	1.130E-06	8.338E-07	-7.297E-07	-5.448E-08	4.093E-07	-1.772E-07	-1.593E-07	2.016E-07	-3.002E-09	-1.405E-07
35	0.70	0.35	-5.737E-06	1.038E-06	9.372E-07	-7.108E-07	-1.313E-07	4.324E-07	-1.307E-07	-2.023E-07	1.877E-07	4.031E-08	-1.537E-07
36	0.72	0.36	-5.950E-06	9.364E-07	1.038E-06	-6.816E-07	-2.100E-07	4.460E-07	-7.747E-08	-2.395E-07	1.639E-07	8.358E-08	-1.569E-07
37	0.74	0.37	-6.162E-06	8.248E-07	1.136E-06	-6.420E-07	-2.892E-07	4.495E-07	-1.894E-08	-2.692E-07	1.308E-07	1.243E-07	-1.494E-07
38	0.76	0.38	-6.374E-06	7.031E-07	1.230E-06	-5.920E-07	-3.675E-07	4.423E-07	4.336E-08	-2.900E-07	8.966E-08	1.601E-07	-1.313E-07
39	0.78	0.39	-6.584E-06	5.715E-07	1.319E-06	-5.319E-07	-4.437E-07	4.242E-07	1.077E-07	-3.007E-07	4.198E-08	1.886E-07	-1.033E-07
40	0.80	0.40	-6.794E-06	4.300E-07	1.403E-06	-4.619E-07	-5.163E-07	3.950E-07	1.723E-07	-3.004E-07	-1.028E-08	2.081E-07	-6.688E-08
41	0.82	0.41	-7.002E-06	2.788E-07	1.479E-06	-3.823E-07	-5.840E-07	3.551E-07	2.353E-07	-2.887E-07	-6.496E-08	2.170E-07	-2.401E-08
42	0.84	0.42	-7.208E-06	1.179E-07	1.549E-06	-2.936E-07	-6.454E-07	3.047E-07	2.946E-07	-2.655E-07	-1.197E-07	2.144E-07	2.283E-08
43	0.86	0.43	-7.413E-06	-5.251E-08	1.610E-06	-1.964E-07	-6.993E-07	2.445E-07	3.486E-07	-2.311E-07	-1.720E-07	1.998E-07	7.081E-08
44	0.88	0.44	-7.617E-06	-2.324E-07	1.663E-06	-9.123E-08	-7.444E-07	1.753E-07	3.953E-07	-1.861E-07	-2.194E-07	1.734E-07	1.169E-07
45	0.90	0.45	-7.818E-06	-4.215E-07	1.706E-06	2.101E-08	-7.796E-07	9.824E-08	4.330E-07	-1.317E-07	-2.596E-07	1.361E-07	1.581E-07
46	0.92	0.46	-8.018E-06	-6.196E-07	1.738E-06	1.395E-07	-8.038E-07	1.450E-08	4.603E-07	-6.936E-08	-2.905E-07	8.928E-08	1.916E-07
47	0.94	0.47	-8.215E-06	-8.267E-07	1.759E-06	2.634E-07	-8.160E-07	-7.444E-08	4.758E-07	-8.426E-10	-3.101E-07	3.491E-08	2.148E-07
48	0.96	0.48	-8.411E-06	-1.043E-06	1.768E-06	3.914E-07	-8.154E-07	-1.669E-07	4.783E-07	7.174E-08	-3.170E-07	-2.453E-08	2.258E-07

49	0.98	0.49	-8.604E-06	-1.267E-06	1.764E-06	5.227E-07	-8.013E-07	-2.612E-07	4.672E-07	1.460E-07	-3.103E-07	-8.622E-08	2.230E-07
50	1.00	0.50	-8.794E-06	-1.499E-06	1.747E-06	6.558E-07	-7.732E-07	-3.554E-07	4.420E-07	2.195E-07	-2.893E-07	-1.470E-07	2.060E-07
51	1.02	0.51	-8.982E-06	-1.740E-06	1.716E-06	7.896E-07	-7.307E-07	-4.474E-07	4.025E-07	2.896E-07	-2.541E-07	-2.037E-07	1.749E-07
52	1.04	0.52	-9.167E-06	-1.988E-06	1.670E-06	9.226E-07	-6.734E-07	-5.352E-07	3.489E-07	3.535E-07	-2.055E-07	-2.530E-07	1.308E-07
53	1.06	0.53	-9.349E-06	-2.244E-06	1.609E-06	1.053E-06	-6.016E-07	-6.166E-07	2.819E-07	4.086E-07	-1.447E-07	-2.919E-07	7.564E-08
54	1.08	0.54	-9.528E-06	-2.507E-06	1.533E-06	1.180E-06	-5.152E-07	-6.894E-07	2.025E-07	4.524E-07	-7.358E-08	-3.177E-07	1.215E-08
55	1.10	0.55	-9.704E-06	-2.777E-06	1.439E-06	1.302E-06	-4.147E-07	-7.517E-07	1.120E-07	4.826E-07	5.473E-09	-3.280E-07	-5.624E-08
56	1.12	0.56	-9.877E-06	-3.053E-06	1.330E-06	1.417E-06	-3.008E-07	-8.012E-07	1.239E-08	4.972E-07	8.952E-08	-3.214E-07	-1.256E-07
57	1.14	0.57	-1.005E-05	-3.336E-06	1.202E-06	1.523E-06	-1.743E-07	-8.361E-07	-9.431E-08	4.946E-07	1.752E-07	-2.970E-07	-1.915E-07
58	1.16	0.58	-1.021E-05	-3.624E-06	1.058E-06	1.619E-06	-3.617E-08	-8.545E-07	-2.055E-07	4.736E-07	2.588E-07	-2.548E-07	-2.497E-07
59	1.18	0.59	-1.037E-05	-3.918E-06	8.950E-07	1.702E-06	1.121E-07	-8.549E-07	-3.185E-07	4.336E-07	3.366E-07	-1.957E-07	-2.958E-07
60	1.20	0.60	-1.053E-05	-4.217E-06	7.141E-07	1.772E-06	2.690E-07	-8.358E-07	-4.300E-07	3.746E-07	4.044E-07	-1.216E-07	-3.259E-07
61	1.22	0.61	-1.069E-05	-4.521E-06	5.147E-07	1.826E-06	4.327E-07	-7.961E-07	-5.368E-07	2.972E-07	4.586E-07	-3.535E-08	-3.368E-07
62	1.24	0.62	-1.084E-05	-4.828E-06	2.966E-07	1.862E-06	6.012E-07	-7.352E-07	-6.354E-07	2.030E-07	4.956E-07	5.924E-08	-3.262E-07
63	1.26	0.63	-1.098E-05	-5.139E-06	5.985E-08	1.878E-06	7.720E-07	-6.525E-07	-7.222E-07	9.379E-08	5.121E-07	1.577E-07	-2.930E-07
64	1.28	0.64	-1.112E-05	-5.454E-06	-1.957E-07	1.874E-06	9.426E-07	-5.481E-07	-7.936E-07	-2.746E-08	5.056E-07	2.547E-07	-2.374E-07
65	1.30	0.65	-1.126E-05	-5.771E-06	-4.701E-07	1.846E-06	1.110E-06	-4.223E-07	-8.461E-07	-1.572E-07	4.744E-07	3.448E-07	-1.612E-07
66	1.32	0.66	-1.139E-05	-6.090E-06	-7.631E-07	1.794E-06	1.272E-06	-2.763E-07	-8.763E-07	-2.914E-07	4.177E-07	4.222E-07	-6.768E-08
67	1.34	0.67	-1.152E-05	-6.410E-06	-1.075E-06	1.715E-06	1.424E-06	-1.114E-07	-8.814E-07	-4.250E-07	3.358E-07	4.810E-07	3.842E-08
68	1.36	0.68	-1.164E-05	-6.732E-06	-1.404E-06	1.608E-06	1.563E-06	7.034E-08	-8.585E-07	-5.529E-07	2.302E-07	5.160E-07	1.509E-07
69	1.38	0.69	-1.176E-05	-7.054E-06	-1.752E-06	1.471E-06	1.686E-06	2.662E-07	-8.056E-07	-6.693E-07	1.036E-07	5.226E-07	2.624E-07
70	1.40	0.70	-1.187E-05	-7.375E-06	-2.117E-06	1.303E-06	1.788E-06	4.730E-07	-7.212E-07	-7.683E-07	-3.977E-08	4.975E-07	3.647E-07
71	1.42	0.71	-1.198E-05	-7.696E-06	-2.498E-06	1.102E-06	1.866E-06	6.867E-07	-6.047E-07	-8.437E-07	-1.944E-07	4.386E-07	4.494E-07
72	1.44	0.72	-1.208E-05	-8.015E-06	-2.896E-06	8.674E-07	1.916E-06	9.028E-07	-4.562E-07	-8.898E-07	-3.536E-07	3.459E-07	5.079E-07
73	1.46	0.73	-1.218E-05	-8.331E-06	-3.309E-06	5.982E-07	1.932E-06	1.116E-06	-2.771E-07	-9.012E-07	-5.093E-07	2.213E-07	5.328E-07
74	1.48	0.74	-1.227E-05	-8.644E-06	-3.736E-06	2.933E-07	1.912E-06	1.321E-06	-6.965E-08	-8.730E-07	-6.526E-07	6.897E-08	5.178E-07

75	1.50	0.75	-1.236E-05	-8.953E-06	-4.177E-06	-4.796E-08	1.851E-06	1.510E-06	1.623E-07	-8.014E-07	-7.740E-07	-1.043E-07	4.590E-07
76	1.52	0.76	-1.243E-05	-9.257E-06	-4.630E-06	-4.260E-07	1.744E-06	1.676E-06	4.136E-07	-6.840E-07	-8.636E-07	-2.893E-07	3.554E-07
77	1.54	0.77	-1.251E-05	-9.556E-06	-5.094E-06	-8.408E-07	1.587E-06	1.813E-06	6.778E-07	-5.198E-07	-9.116E-07	-4.746E-07	2.093E-07
78	1.56	0.78	-1.257E-05	-9.848E-06	-5.567E-06	-1.292E-06	1.378E-06	1.911E-06	9.466E-07	-3.101E-07	-9.092E-07	-6.467E-07	2.734E-08
79	1.58	0.79	-1.263E-05	-1.013E-05	-6.048E-06	-1.780E-06	1.111E-06	1.962E-06	1.210E-06	-5.831E-08	-8.486E-07	-7.905E-07	-1.799E-07
80	1.60	0.80	-1.269E-05	-1.041E-05	-6.534E-06	-2.303E-06	7.838E-07	1.956E-06	1.457E-06	2.292E-07	-7.243E-07	-8.903E-07	-3.971E-07
81	1.62	0.81	-1.274E-05	-1.067E-05	-7.024E-06	-2.860E-06	3.937E-07	1.885E-06	1.674E-06	5.433E-07	-5.338E-07	-9.305E-07	-6.053E-07
82	1.64	0.82	-1.278E-05	-1.093E-05	-7.516E-06	-3.450E-06	-6.165E-08	1.740E-06	1.847E-06	8.711E-07	-2.783E-07	-8.969E-07	-7.819E-07
83	1.66	0.83	-1.281E-05	-1.117E-05	-8.006E-06	-4.069E-06	-5.839E-07	1.511E-06	1.959E-06	1.196E-06	3.622E-08	-7.785E-07	-9.025E-07
84	1.68	0.84	-1.284E-05	-1.140E-05	-8.493E-06	-4.714E-06	-1.174E-06	1.190E-06	1.993E-06	1.499E-06	3.981E-07	-5.687E-07	-9.427E-07
85	1.70	0.85	-1.286E-05	-1.162E-05	-8.972E-06	-5.383E-06	-1.830E-06	7.685E-07	1.932E-06	1.756E-06	7.891E-07	-2.680E-07	-8.803E-07
86	1.72	0.86	-1.288E-05	-1.182E-05	-9.442E-06	-6.071E-06	-2.552E-06	2.406E-07	1.756E-06	1.938E-06	1.184E-06	1.145E-07	-6.993E-07
87	1.74	0.87	-1.289E-05	-1.201E-05	-9.898E-06	-6.772E-06	-3.336E-06	-3.990E-07	1.447E-06	2.017E-06	1.549E-06	5.585E-07	-3.929E-07
88	1.76	0.88	-1.289E-05	-1.218E-05	-1.034E-05	-7.479E-06	-4.177E-06	-1.153E-06	9.878E-07	1.957E-06	1.842E-06	1.030E-06	3.120E-08
89	1.78	0.89	-1.289E-05	-1.233E-05	-1.075E-05	-8.186E-06	-5.068E-06	-2.022E-06	3.630E-07	1.724E-06	2.015E-06	1.482E-06	5.462E-07
90	1.80	0.90	-1.289E-05	-1.246E-05	-1.114E-05	-8.884E-06	-5.998E-06	-3.002E-06	-4.391E-07	1.285E-06	2.011E-06	1.847E-06	1.101E-06
91	1.82	0.91	-1.287E-05	-1.256E-05	-1.150E-05	-9.563E-06	-6.955E-06	-4.083E-06	-1.425E-06	6.054E-07	1.769E-06	2.047E-06	1.618E-06
92	1.84	0.92	-1.286E-05	-1.265E-05	-1.182E-05	-1.021E-05	-7.922E-06	-5.252E-06	-2.594E-06	-3.390E-07	1.228E-06	1.985E-06	1.985E-06
93	1.86	0.93	-1.284E-05	-1.272E-05	-1.210E-05	-1.081E-05	-8.878E-06	-6.484E-06	-3.933E-06	-1.563E-06	3.303E-07	1.558E-06	2.064E-06
94	1.88	0.94	-1.281E-05	-1.276E-05	-1.233E-05	-1.136E-05	-9.796E-06	-7.746E-06	-5.414E-06	-3.064E-06	-9.654E-07	6.637E-07	1.692E-06
95	1.90	0.95	-1.279E-05	-1.278E-05	-1.251E-05	-1.182E-05	-1.064E-05	-8.993E-06	-6.988E-06	-4.809E-06	-2.671E-06	-7.785E-07	7.013E-07
96	1.92	0.96	-1.277E-05	-1.278E-05	-1.263E-05	-1.220E-05	-1.138E-05	-1.016E-05	-8.576E-06	-6.723E-06	-4.743E-06	-2.797E-06	-1.040E-06
97	1.94	0.97	-1.275E-05	-1.276E-05	-1.270E-05	-1.246E-05	-1.197E-05	-1.117E-05	-1.006E-05	-8.669E-06	-7.055E-06	-5.316E-06	-3.561E-06
98	1.96	0.98	-1.273E-05	-1.274E-05	-1.271E-05	-1.261E-05	-1.236E-05	-1.193E-05	-1.129E-05	-1.041E-05	-9.325E-06	-8.049E-06	-6.633E-06
99	1.98	0.99	-1.273E-05	-1.272E-05	-1.270E-05	-1.266E-05	-1.256E-05	-1.239E-05	-1.212E-05	-1.174E-05	-1.122E-05	-1.056E-05	-9.760E-06
100	2.00	1.00	-1.273E-05	-1.272E-05	-1.272E-05	-1.270E-05	-1.267E-05	-1.261E-05	-1.253E-05	-1.241E-05	-1.224E-05	-1.203E-05	-1.175E-05